Neural Networks 26 (2012) 29–58

Contents lists available at SciVerse ScienceDirect

Neural Networks

journal homepage: www.elsevier.com/locate/neunet

A neural model of sequential movement planning and control of eye movements: Item-Order-Rank working memory and saccade selection by the supplementary eye fields

Matthew R. Silver [a,b,c], Stephen Grossberg [a,b,c,*], Daniel Bullock [a,b,c], Mark H. Histed [c,d,e,f], Earl K. Miller [c,d,e]

[a] Center for Adaptive Systems, Boston University, Boston, MA 02215, United States
[b] Department of Cognitive and Neural Systems, Boston University, Boston, MA 02215, United States
[c] Center of Excellence for Learning in Education, Science, and Technology, Boston University, Boston, MA 02215, United States
[d] The Picower Institute for Learning and Memory, Massachusetts Institute of Technology, Cambridge, MA 02139, United States
[e] Department of Brain and Cognitive Sciences, Massachusetts Institute of Technology, Cambridge, MA 02139, United States
[f] Department of Neurobiology, Harvard Medical School, Boston, MA 02115, United States

ARTICLE INFO

Article history:
Received 30 December 2010
Received in revised form 22 September 2011
Accepted 12 October 2011

Keywords:
Working memory
Saccade
Planning
Rank-order coding
Counting
Movement choice
Immediate serial recall
Basal ganglia
Prefrontal cortex
Supplementary eye fields
Parietal cortex
Frontal eye fields
Superior colliculus

ABSTRACT

How does working memory store multiple spatial positions to control sequences of eye movements, particularly when the same items repeat at multiple list positions, or ranks, during the sequence? An Item-Order-Rank model of working memory shows how rank-selective representations enable storage and recall of items that repeat at arbitrary list positions. Rank-related activity has been observed in many areas including the posterior parietal cortices (PPC), prefrontal cortices (PFC) and supplementary eye fields (SEF). The model shows how rank information, originating in PPC, may support rank-sensitive PFC working memory representations and how SEF may select saccades stored in working memory. It also proposes how SEF may interact with downstream regions such as the frontal eye fields (FEF) during memory-guided sequential saccade tasks, and how the basal ganglia (BG) may control the flow of information. Model simulations reproduce behavioral, anatomical and electrophysiological data under multiple experimental paradigms, including visually- and memory-guided single and sequential saccade tasks. Simulations reproduce behavioral data during two SEF microstimulation paradigms, showing that their seemingly inconsistent findings about saccade latency can be reconciled.

1. Introduction

Short term sequential storage, or working memory (WM), has emerged as a critical probe of the brain's memory capacities. Tests of immediate serial recall (ISR), in which subjects are presented with a list of items and subsequently asked to reproduce the items in order, have advanced our understanding of the neural bases of memory. As data accumulated from studies involving ISR and similar tasks, models of WM were developed to explain them. Lashley (1951) suggested that items are retained in parallel in spatially separable neural populations, thus transforming the temporal problem of serial order into a spatial problem. Grossberg (1978a, 1978b) developed a neural model of WM through which a temporal stream of inputs could be stored as an evolving spatial pattern before being performed sequentially during rehearsal. In such an Item-and-Order WM, individual nodes, or cell populations, represent *list items*, and the order in which the items were presented is stored by an *activity gradient* across these nodes. A *primacy gradient* achieves performance in the correct temporal order. In a primacy gradient, the first item in the sequence is represented by the node with the highest activity, the node representing the second item in the sequence has the second highest activity, and so on, until all items in the sequence are represented. A rehearsal wave enables read-out of these activities when it is time to reproduce the sequence. The node with the highest activity is read out first and self-inhibits its

* Corresponding author at: Center for Adaptive Systems, Boston University, 677 Beacon Street, Boston, MA 02215, United States. Tel.: +1 617 353 7857; fax: +1 617 353 7755.
E-mail address: steve@bu.edu (S. Grossberg).

0893-6080/$ – see front matter © 2011 Elsevier Ltd. All rights reserved.
doi:10.1016/j.neunet.2011.10.004

WM representation, an example of an *inhibition of return*, which prevents perseveration. This process is repeated until the entire sequence is reproduced and there are no active nodes in the WM.

Since the introduction of the Item-and-Order WM, which is also known as competitive queuing (CQ; Houghton, 1990), many models have built upon it (Boardman & Bullock, 1991; Bohland, Bullock, & Guenther, 2010; Bradski, Carpenter, & Grossberg, 1994; Bullock & Rhodes, 2003; Grossberg & Pearson, 2008; Houghton, 1990; Page & Norris, 1998). Electrophysiological recordings from prefrontal cortex (PFC) have supported the prediction by Grossberg (1978a, 1978b) that neural ensembles represent list items, encode the order of the items with their relative activity levels, and are reset by self-inhibition; e.g. Averbeck, Chafee, Crowe, and Georgopoulos (2002).

Most CQ implementations utilize a localist representation of list items: single nodes, representing populations of neurons, become active in response to the presentation of specific items. In its simplest form, this kind of item representation cannot represent the same item in multiple positions, or ranks, of a list. However, the activity of PFC neurons for a given list item is sometimes modulated by the rank of that item within the sequence (Averbeck, Chafee, Crowe, & Georgopoulos, 2003; Barone & Joseph, 1989; Mushiake, Saito, Sakamoto, Itoyama, & Tanji, 2006). In addition, error data imply utilization of rank information in serial recall (e.g. Bowman & Wyble, 2007; Conrad, 1960; Henson, 2001), which some models of serial recall have incorporated (Brown, Preece, & Hulme, 2000; Burgess & Hitch, 1999; Henson, 1998).

Despite some positive results from rank-based models, Farrell and Lewandowsky (2004) have shown that latency data from error trials can be best explained by models that use a primacy gradient and self-inhibition (i.e., Item-and-Order models), but not by those that use rank alone. Some CQ models have incorporated rank information (Bohland et al., 2010; Bradski et al., 1994). The LIST PARSE model of Grossberg and Pearson (2008) has proposed how rank-order coding can be incorporated into an Item-and-Order WM in PFC to represent repeats at arbitrary list positions based upon representations of numerosity in posterior parietal cortex (PPC). This article builds upon their proposal to present an *Item-Order-Rank* model of WM storage and performance that, for the first time, uses rank information to quantitatively simulate neurobiological data about rank-order coding in a spatial WM (Fig. 1).

The model proposes how item representations are chosen from WM by the supplementary eye field (SEF), an oculomotor area in dorsomedial frontal cortex (Schlag & Schlag-Rey, 1987) which is heavily interconnected with the PFC (Barbas & Pandya, 1987; Huerta & Kaas, 1990) and which also exhibits rank-related activity (Berdyyeva & Olson, 2009; Isoda & Tanji, 2002, 2003). SEF is thus anatomically and physiologically well-suited to interact with a rank-selective WM, and has long been thought to be important in the production of memory-guided saccade sequences, as evidenced by investigations that explored oculomotor deficits in patients with lesions in what was at the time called the supplementary motor area (Gaymard, Pierrot-Deseilligny, & Rivaud, 1990; Gaymard, Rivaud, & Pierrot-Deseilligny, 1993). In these studies, performance was mostly intact for visually-guided saccades, antisaccades, and single memory-guided saccades, but greatly degraded for *sequences* of memory-guided saccades.

The importance of SEF for the production of memory-guided saccade sequences has been confirmed through lesion studies (Schiller & Chou, 1998) and reversible inactivation (Sommer & Tehovnik, 1999) in monkeys. Moreover, activation of SEF during sequential saccade tasks has been observed with positron emission tomography (Petit et al., 1996) and during a functional magnetic resonance imaging study (Heide et al., 2001) whose authors concluded that "the supplementary eye field essentially controls the triggering of memorized saccade sequences". More recently, researchers have hypothesized that SEF resolves conflicts between plans, or selects actions (Berdyyeva & Olson, 2009; Nachev, Rees, Parton, Kennard, & Husain, 2005; Parton et al., 2007; So & Stuphorn, 2010), consistent with our hypothesis that SEF selects saccade plans from spatial WM.

In addition to processes of numerosity in PPC, spatial WM storage in PFC, and saccade selection in SEF, the model clarifies how the basal ganglia (BG) selectively gate the release of a saccadic movement only when a frontal–parietal resonance develops that embodies a system consensus about a chosen saccade command (Fig. 1). How the BG realize such a resonant consensus was described in the TELOS model of Brown, Bullock, and Grossberg (2004). The model's integration and elaboration of LIST PARSE WM and TELOS gated choice explains the name, lisTELOS, of the current model.

The competence of the lisTELOS model was tested within a variety of different paradigms including visually-guided and memory-guided saccade tasks and several sequential saccade tasks, notably the ISR task. The model is compatible with known anatomical data, and reproduces behavioral and electrophysiological data under a variety of conditions, including those in which SEF activity is perturbed by microstimulation (Histed & Miller, 2006; Yang, Heinen, & Missal, 2008).

2. Methods

The lisTELOS model utilizes rank-related activity to build an Item-and-Order working memory (WM) system that can reproduce sequences of saccades with items repeated at arbitrary ordinal positions; that is, an Item-Order-Rank WM system. The model describes multiple interacting cortical and subcortical areas, including parietal and prefrontal cortices, the frontal and supplementary eye fields, multiple basal ganglia loops, and superior colliculus. The model is comprised of multiple populations of cells representing each of these brain areas. Neuronal firing rates are simulated as continuous variables, and at several points, the model incorporates competition through local inhibition, resulting in realistic temporal dynamics. The model's mathematical specification is given in Section 4.

2.1. Posterior parietal cortex: cue onset detection and rank activity

When a cue is presented to the model, it first excites cells in area 7*a* of posterior parietal cortex (PPC); see Fig. 1. Three populations of 7*a* cells interact to produce a signal that marks cue onsets with a transient burst of activity. Cue inputs I_i (Eq. (2)) first excite a population of excitatory cells with activity levels P_i^X (Eq. (5)) that respond strongly for the duration of the cue's presence. These cells excite interneurons with activities P_i^I which also track inputs (Eq. (6)). Both of these populations project to a third population of transient onset cells whose activity levels P_i^Y are high immediately following cue presentation but subsequently equilibrate at lower levels (Eq. (8)). A transient onset response is generated because of the balance between the converging excitatory and inhibitory signals P_i^X and P_i^I, respectively. Transient onset cell activities P_i^Y serve as the driving input to PFC WM cells, with activity levels M_{ir}, as described in Section 2.2. Also contained within the model PPC is a population of lateral intraparietal (LIP) cells with activities P_i^L (Eq. (9)) that are excited by area 7*a* activities P_i^Y. These cells retain representations of cues present in the environment that compete with each other, and with cues represented by FEF cell activities F_i^O that help to store planned saccades. As described in Section 2.5, LIP cells and FEF cells must reach a consensus about the saccade to be executed before saccade production.

Model PPC *counting cell* activities P_r^C are sensitive to a preferred rank, r; see Section 4.5. Rank-related activity, characterized by

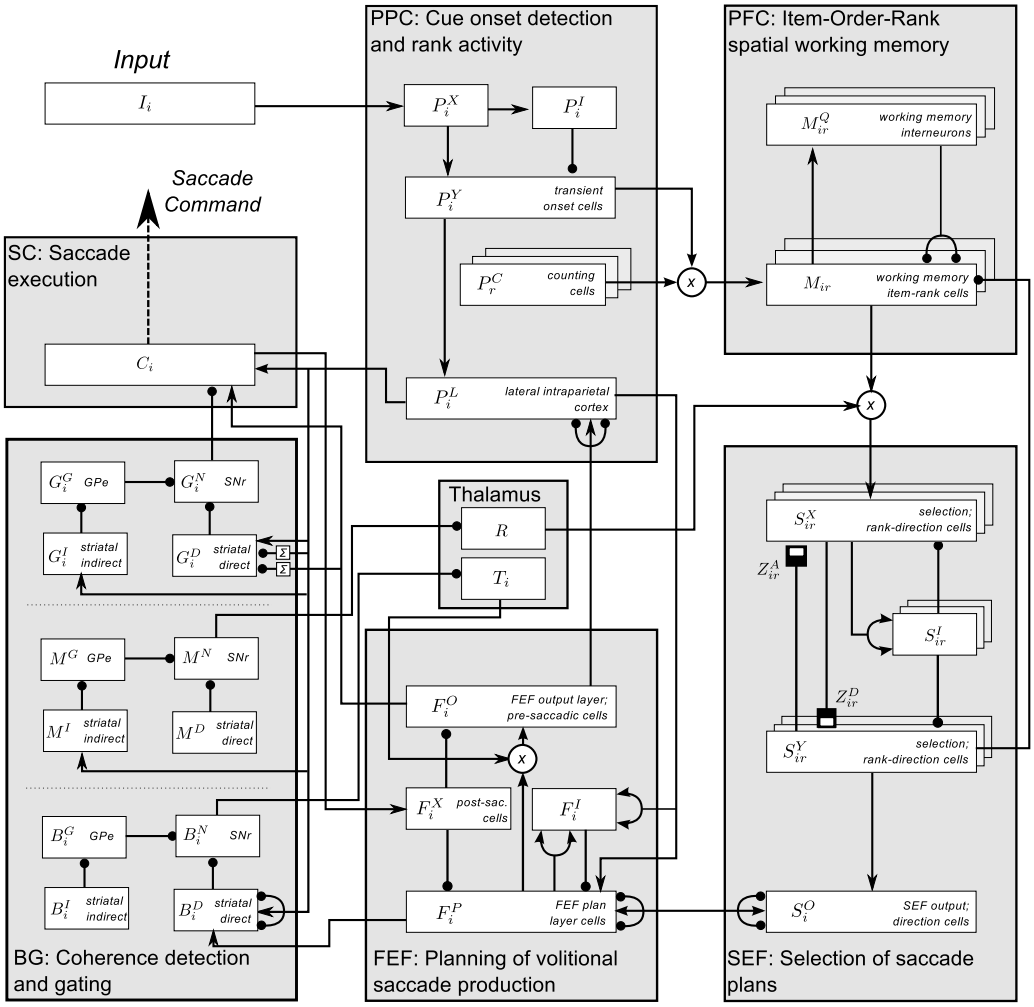

Fig. 1. An Item-Order-Rank spatial working memory and performance model. Each gray box represents a brain region within which fields of cells, represented by white inset boxes, share similar functional roles. Arrowheads denote excitatory connections between cells, and filled circles represent inhibitory connections. Curved branches at the ends of connections represent one-to-many fan-out connections that impact all other cells in the field. Half-filled boxes at the ends of connections represent habituative gates which exhibit activity-dependent changes in synaptic efficacy. White circles containing a multiplication sign ($\times$) represent multiplicative interaction between two signals. Boxes containing a sigma (Σ) represent the sum of outputs from all cells in the field that gave rise to the projection. Stacked field representations denote populations of rank-sensitive cells.

changes in firing rate that depend upon the ordinal position of a stimulus within a sequence, has been observed in several brain areas, including PFC (Averbeck et al., 2003; Barone & Joseph, 1989; Mushiake et al., 2006), SEF (Berdyyeva & Olson, 2009; Isoda & Tanji, 2002, 2003), and PPC (Nieder, Diester, & Tudusciuc, 2006; Sawamura, Shima, & Tanji, 2002). Rank coding may arise in PPC, which is known to be involved with the representation of numerosity (Dehaene, 1997; Dehaene, Spelke, Pinel, Stenescu, & Tsivkin, 1999; Grossberg & Repin, 2003). Behavioral studies have demonstrated that monkeys can order stimulus arrays on the basis of the number of stimuli contained in each array (Brannon & Terrace, 1998, 2000; Nieder & Miller, 2004a). Nieder and Miller (2004b) observed that, in a delayed match to numerosity task, cells near the intraparietal sulcus are selective for particular numerosities. Roitman, Brannon, and Platt (2007) observed similar LIP activity in a numerosity discrimination task. These numerosity-selective cells are broadly tuned: their activity is maximal when an array with the preferred numerosity is presented and, when stimulus arrays with non-preferred numerosity are presented, cell activity varies as a decreasing function of the difference between the new and preferred numerosities, properties that were simulated in the model by Grossberg and Repin (2003).

These studies sought to characterize neural activity when numerosity is conveyed in a *spatial* way. Parts of PPC have also been observed to exhibit numerosity-selectivity in the *temporal* domain. Sawamura et al. (2002) demonstrated that cells in the superior parietal lobule (SPL) are able to "count" the number of movements a monkey makes. In their study, monkeys were trained to produce two types of arm movements. To receive reward, monkeys had to produce exactly five consecutive movements of one type, switch to the other type, perform five movements, switch back to the first, and continue. Counting cells fired most before movements of a given ordinal position, and were broadly tuned, much like the spatial numerosity cells described above. Nieder et al. (2006) recorded activity of PPC cells during a traditional spatial numerosity task and during a temporal counting task, wherein monkeys watched as a cue was presented n times and then indicated whether or not a subsequent stimulus array had numerosity equal to n. Their results showed that the population of cells representing numerosity in the temporal task, presumed to be similar to the counting cells described by Sawamura et al. (2002), is separate from that which responds during a spatial task.

Taken together, these results indicate that multiple separable populations of cells in the intraparietal sulcal region of PPC contain representations of numerical values. Such cells represent the numerosity of stimuli, and can "count" events that unfold in time. In model simulations, each time a non-fixation-related cue is presented, the counting cell population with activities P_r^C is updated:

Table 1
Counting cell activities P_r^C for each rank. These population activities correspond to a system with three counting cells.

Rank	Counting cell population
1	$P^C = \langle 1\,0\,0 \rangle$
2	$P^C = \langle 0\,1\,0 \rangle$
3	$P^C = \langle 0\,0\,1 \rangle$

when the first cue is presented, the cell with preferred rank $r = 1$ is activated and all others silenced, when the second cue is presented the cell with a preferred rank $r = 2$ is activated, and so on, as described by Table 1. Building on the proposal of Grossberg and Pearson (2008), our model uses counting cell activity to produce rank-related activity in PFC and SEF, both recipients of PPC projections (Petrides & Pandya, 1984). Further support for this hypothesis has been offered by Nieder and Miller (2004b) who observed that numerosity information appears earlier in PPC than PFC.

In summary, when a cue is presented to the model, it excites transient stimulus onset activities P_i^Y, and counting cell activities P_r^C that behave in a manner similar to the SPL cells observed by Sawamura et al. (2002). Together, these cell activities contain information encoding both a cue's spatial position (7*a* cell activities P_i^Y) and ordinal position, or rank (SPL cell activities P_r^C).

2.2. Prefrontal cortex: Item-Order-Rank spatial working memory

Both of the above PPC populations project to model PFC cells with activities M_{ir} (Eq. (12) and Fig. 1), where subscript r again denotes preferred rank. The recipient PFC cells implement an Item-Order-Rank WM. As items are instated into WM, they inhibit other cells in the WM through interneuron activities M_{ir}^Q(Eq. (16)) so that, when future items are added to memory, the new representations are weaker. With each cue, the total amount of inhibition increases so that it is progressively more difficult to strongly activate cells. Under the correct conditions, this creates a finite-capacity WM that represents sequences with a primacy gradient (Bradski et al., 1994).

The two sources of input to PFC combine so that the item representation that is instated into WM is a conjunction of the cue's spatial position and rank (Fig. 2(A)). This representation allows cues presented at the same spatial position, which share the same *item* information, to be differentiated on the basis of their *rank* within position-rank 'hypercolumns'. Sequences with items repeated at arbitrary ordinal positions can hereby be stored and performed. The combination of rank-dependent representations and the Item-and-Order WM's activity gradient together produce an Item-Order-Rank spatial WM in which the order of the sequence is redundantly coded, both within the activity gradient and the item representations themselves (Fig. 2(B)).

The convergent inputs from PPC are gated by a parameter μ(Eq. (13)) that can stop PPC cells from exciting WM cells M_{ir}. Through this parameter, the WM can be removed from the model on tasks that do not require storage of visual information, consistent with data demonstrating that PFC WM cells do not fire during such tasks (Fuster, 1973; Kojima & Goldman-Rakic, 1984). Our use of this parameter provides a simple representation of a neural mechanism that controls the information allowed to be stored in working memory, as suggested by the observation that, given the presentation of identical stimuli, neural selectivity in PFC depends on subsequent task demands (Warden & Miller, 2010). Awh and Vogel (2008), describing imaging data from McNab and Klingberg (2008), observed that variation among individuals on success in WM tasks could be associated, not with WM capacity limitations, but rather with the ability of individuals to selectively identify and store task-related stimuli. Tsushima, Seitz, and Watanabe (2008) showed that the presence of subliminal distractors damages performance in attention tasks, but that bringing distractors above threshold alleviates performance deficits, indicating that the ability to filter out distracting stimuli leads to direct improvements in performance. It is possible that the brain learns to 'blacklist' distracting stimuli, allowing all other information to be stored. However, it is also possible that, when performance does not depend on WM, all stimuli are blacklisted while representations that may later be identified as important can be selectively allowed to flow into WM. The parameter μ, set to 0 at the beginning of non-WM tasks to stop the flow of information into the model WM, represents such a learned competency.

2.3. Supplementary eye field: selection of saccade plan

Once a sequence has been stored in an Item-Order-Rank WM, it is reproduced through the model SEF which iteratively selects, and then deletes, the most active representation. The model clarifies data suggesting that the medial frontal cortices, of which SEF is a part, play a role in conflict resolution or action selection (Nachev et al., 2005; Parton et al., 2007; So & Stuphorn, 2010; Taylor, Nobre, & Rushworth, 2007). In particular, the model SEF contains a winner-take-all network that selects the most active representation among those represented by WM cell activities M_{ir}. The winner-take-all SEF network in the model utilizes three key processes to perform the selection: recurrent competition, feedforward competition, and habituative gating. The competitive network is composed of two excitatory layers with cell activities S_{ir}^X and S_{ir}^Y, and an inhibitory layer with cell activities S_{ir}^I (Eqs. (18), (22) and (20), respectively). The feedforward competition is implemented through one-to-one connections between the two excitatory layers and divergent off-surround signals that excite interneuron activities S_{ir}^I to inhibit cells that represent all dissimilar spatial positions. The recurrent competition uses a one-to-one excitatory feedback from the second selection layer to the first layer, and off-surround inhibitory feedback through the activity S_{ir}^I of the same population of interneurons. Finally, the reciprocal excitatory connections between the two layers are controlled by habituative gates Z_{ir}^A and Z_{ir}^D (Eqs. (19) and (23)) that introduce local activity-dependent reductions in synaptic efficacy (Grossberg, 1968, 1972). When cells between the two layers strongly excite one another, as must occur to win the competition, their synapses habituate in response to the high level of activation, which correspondingly reduces signal strength. This process weakens representations after they have won the competition. Without such a process, the recurrent excitatory connections between the two layers could allow the winning cells to excite each other permanently, leading the system to perseverate on a single saccade plan.

Once the most active representation in WM has been selected, its representation is deleted by strong inhibitory feedback from SEF cell activities S_{ir}^Y to corresponding WM cell activities M_{ir}. Simultaneously, the rank information is removed from the winning representation as a corresponding rank-*insensitive* representation is excited in SEF output cell activities S_i^O (Eq. (24)). SEF output cells then excite a representation of the selected plan, mapped into retinotopic coordinates, in FEF plan cell activities F_i^P. As described in the following sections, the representation that is introduced into FEF serves as a saccade plan that sends bids to the basal ganglia (BG), which opens thalamic and superior colliculus (SC) gates to execute the plan.

The model reproduces observed behavioral responses in both the presence and absence of SEF microstimulation. During tasks in which microstimulation is applied, including the Histed and Miller (2006) and Yang et al. (2008) tasks, all SEF cells

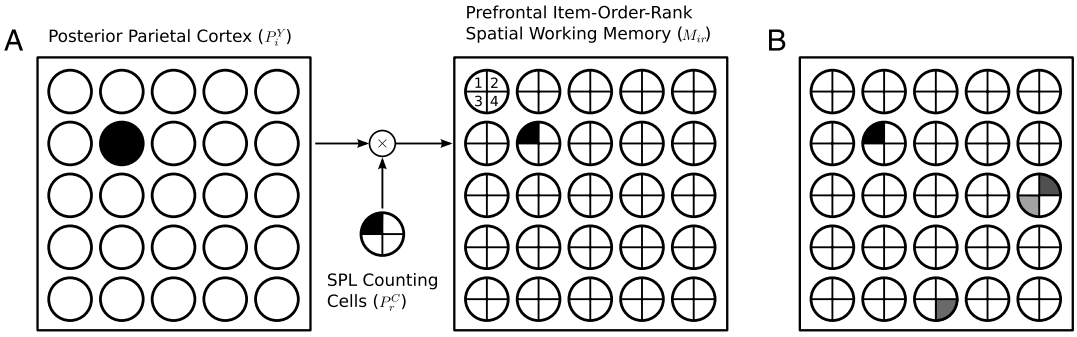

Fig. 2. Counting cells combine with item representations to create rank-sensitive working memory. When cues are instated into working memory, they are bound with rank information so that the instated item is a conjunction of spatial position and ordinal position. (A) The first cue is presented, represented by the darkened cell in PPC, and the first rank cell is active, shown by the darkened wedge among the four SPL cells. The spatial position information contained in PPC and the rank information contained in SPL combine so that only one cell in one working memory hypercolumn is activated. (B) Representation of a sequence of spatial cues in which one spatial position was cued twice during the sequence. Order information is encoded redundantly in an Item-Order-Rank working memory, both explicitly through rank-selective cells within hypercolumns corresponding to spatial positions, and through activation level, represented by the shade of gray.

(Eqs. (18), (20), (22) and (24)) are excited to some degree. In the model, microstimulation is implemented through an additional shunted excitatory term ς_i whose values are determined by a two-dimensional spatial Gaussian function centered over the microstimulation location (Eq. (26)). While microstimulation might activate a small number of cells in other areas, since microstimulation primarily activates neurons whose axons pass close to the microelectrode tip (Histed, Bonin, & Reid, 2009) and are therefore not necessarily local, the average distribution of local activated cells is likely to be Gaussian, especially over 1 mm or more, the approximate scale of our SEF topography. Because a Gaussian is used to model the effect of microstimulation, cells closest to the microstimulation site are excited most strongly while more distant cells receive less or no excitation.

Microstimulation can alter model behavior in two ways: First, by directly exciting SEF cells, microstimulation reorganizes the impact of recurrent competition across SEF (Eq. (24)) and weakly excites FEF via SEF (Eq. (27)). Second, microstimulation can lead to a sustained weakening of synapses with habituative gates Z_{ir}^A and Z_{ir}^D (Eqs. (18) and (22)). As microstimulation excites cells, synapses habituate in an activity-dependent way, so that portions of the network can be rendered less responsive during later stages of the task. The level of habituation depends on both the duration of microstimulation, and proximity to the stimulation site. Because synapses of cells close to the stimulation site are most activated by microstimulation, they become most strongly habituated, leading to a Gaussian-shaped habituative gradient following microstimulation offset.

2.4. Frontal eye field: planning of volitional saccade production

Saccade plans that have been selected by SEF excite corresponding plans represented by cell activities F_i^P in the FEF *plan layer* (Eq. (27)), the first of two excitatory layers (Fig. 3) in the model FEF. FEF plan layer cell activities F_i^P retain the selected plan until task conditions allow for the production of the saccade. This sustained activity enables preparation for a plan before it is executed. To execute the plan, FEF plan layer cell activities F_i^P must activate FEF *output layer* cell activities F_i^O (Eq. (31)), but cannot do so until a BG gate opens and renders the output layer cells responsive to plan layer signals (Brown et al., 2004). Gate opening occurs when FEF plan layer cell activities F_i^P (Eq. (27)) and LIP cell activities P_i^L (Eq. (9)) reach a consensus. Consensus occurs when the two fields activate the same saccade plan, which occurs as a result of cooperation between the fields (Brown et al., 2004; Buschman & Miller, 2007) and competition that is mediated by FEF interneuron activities F_i^I (Eq. (28)). Output layer cells then activate superior colliculus (SC) cell activities C_i (Eq. (32)) which generate saccades. The opening of another BG gate is required before these SC cells can be excited (Hikosaka & Wurtz, 1983); see term G_i^N in Eq. (32). Once a saccade is generated, the SC sends inhibitory feedback to FEF through postsaccadic cell activities F_i^X (Eq. (29)), which inhibit cells in both the plan and output layers. For simplicity, the thalamic stage presumed to mediate SC-to- FEF feedback is omitted.

2.5. Basal ganglia: coherence detection and gating

The model uses three loops through the BG (Middleton & Strick, 2000) to control the flow of information between model areas (Fig. 4). Each of these loops is based on the BG implementation used in the TELOS model of Brown et al. (2004) which explains how the BG can balance between the production of planned and reactive saccades. In TELOS, as has been hypothesized by other researchers (Alexander & Crutcher, 1990; Bullock & Grossberg, 1988, 1991; Gancarz & Grossberg, 1999; Grossberg, Roberts, Aguilar, & Bullock, 1997; Hikosaka & Wurtz, 1983; Mink, 1996), the BG are responsible for controlling movements through a gating process. Eye movements are initiated when consistent saccade plans in FEF and PPC occur, thereby changing the balance of excitation and inhibition impinging on the BG in favor of selective gate opening. By ensuring that these areas reach consensus before allowing saccade generation, the BG avoid various problems such as premature execution of reactive saccades when a planned saccade is appropriate, or simultaneous execution of multiple saccade plans, as sometimes occurs in the form of saccadic averaging (Lee, Rohrer, & Sparks, 1988; Ottes, Van Gisbergen, & Eggermont, 1984).

BG gate opening in the model relies on opposing forces between the direct and indirect pathways (Brown et al., 2004; Frank, 2005; Frank, Loughry, & O'Reilly, 2001; Mink, 1996). The direct and indirect pathways begin with two distinct populations of γ-aminobutyric acid (GABA) releasing medium spiny projection neurons (MSPNs) in the striatum, the input nucleus of the BG. These pathways differentially express D1 and D2 receptors (Gerfen et al., 1990; Surmeier, Ding, Day, Wang, & Shen, 2007). In particular, MSPNs in the direct pathway send projections directly to the globus pallidus internal segment (GPi) and the substantia nigra pars reticulata (SNr), which serve as output nuclei of the BG. Cells in GPi/SNr are GABAergic and tonically inhibit cells in the thalamus or SC (Bullock & Grossberg, 1991; Hikosaka & Wurtz, 1983; Horak & Anderson, 1984). Activation of direct pathway MSPNs inhibits GPi/SNr cells, and thereby disinhibits cells recipient of the tonic GPi/SNr signal.

Indirect pathway MSPNs, rather than inhibiting GPi/SNr, inhibit cells in the nearby globus pallidus external segment (GPe) which,

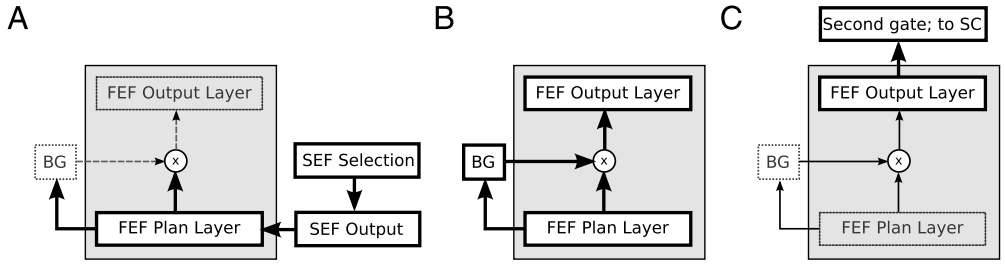

Fig. 3. FEF plan layer and output layer interaction. In order for plans to move through the layers in FEF, so that they can ultimately excite SC and produce a saccade, BG gates must be opened. There are two BG loops that interact with FEF cells to control the flow of information through the region. (A) SEF has selected a saccade plan and excites cells in the FEF plan layer. Plan layer cells try to excite output layer cells but cannot do so when the gate is closed because of a multiplicative interaction between BG output (through the thalamus) and FEF plan layer signals. (B) FEF plan cells activate the BG's direct pathway and open the gate, which allows the plan to be excited in the output layer. (C) Plans in the output layer go through the same process to excite SC.

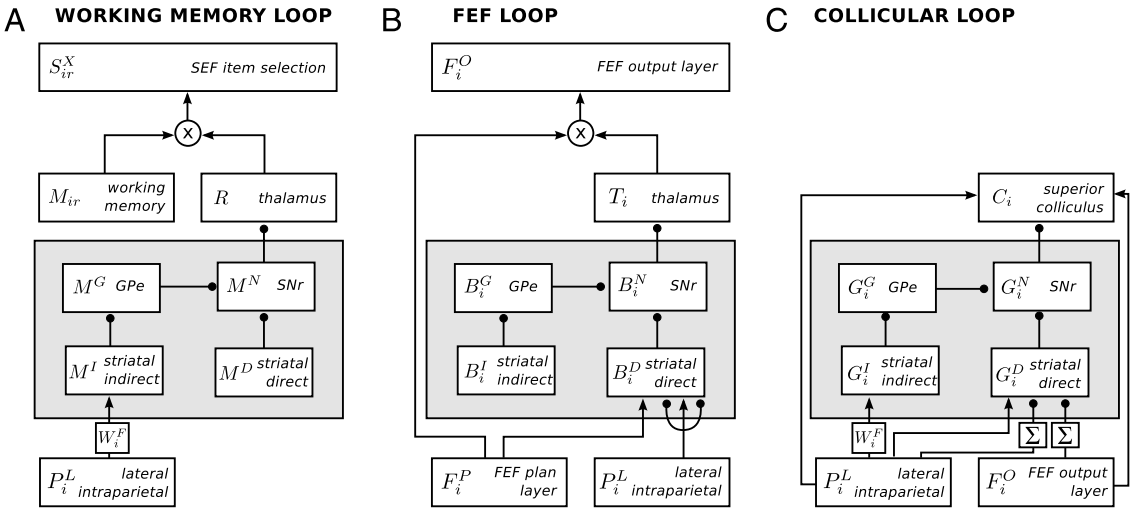

Fig. 4. Three loops through the basal ganglia. The model has three loops through the BG, each of which projects to a separate thalamic or collicular population, modulating the population's excitability and thereby controlling the flow of information from one model stage to another. (A) The left panel represents the working memory loop through the BG, which is responsible for controlling the flow of information from working memory cell activities M_{ir}, to the SEF selection cell activities S^X_{ir}. (B) The FEF loop controls the flow of plan signals from FEF plan layer cell activities F^P_i to FEF output layer cell activities F^O_i. (C) The collicular loop controls excitation of SC cell activities C_i, by FEF output cell activities F^O_i, and LIP cell activities P^L_i.

in turn, inhibit the GPi/SNr output nuclei. Thus, exciting indirect pathway MSPNs disinhibits GPi/SNr cells. The resulting increased activity of GPi/SNr inhibits SC or thalamic cells. As a result, the indirect pathway acts in opposition to the direct pathway: Whereas direct pathway activation excites cells in thalamus or SC, indirect pathway activation inhibits them. The opposing processes of disinhibition and inhibition, which ultimately lead to facilitation or suppression of other neural processes, respectively, are often referred to as *gating*.

The model contains three parallel loops through the BG, each of which is responsible for gating a separate process. The BG WM loop (Fig. 4(A)) is used to control the flow of information from PFC WM cell activities M_{ir} to SEF selection cell activities S^X_{ir} through the thalamic rehearsal gate R (Eq. (38)). Using a set of hard-coded weights W^F_i (Eq. (35)) between LIP cell activities P^L_i and MSPNs of the indirect pathway, with activities M^I (Eq. (34)), the model responds selectively to the presence of a fixation cue by inhibiting indirect pathway GPe cell activities M^G (Eq. (36)) and thereby disinhibiting SNr cell activities M^N (Eq. (37)). The resulting increased SNr activity holds the WM rehearsal gate R closed, restricting the flow of information into SEF. Once the fixation point has been removed, LIP cell activities P^L_i no longer excite MSPNs, and the rehearsal gate opens, allowing SEF cell activities S^X_{ir} to be activated by WM cell activities M_{ir}. As long as no future instances of fixation occur, the gate will remain open and each of the saccade plans can be successively selected and then instated into downstream areas, FEF and ultimately SC, for execution. Direct pathway MSPN activities M^D (Eq. (33)) have a constant activity so that, in the absence of indirect pathway activity, the WM rehearsal gate R is open.

A second BG loop, the FEF loop (Fig. 4(B)), controls the flow of information between the two excitatory populations in FEF: plan layer cell activities F^P_i and output layer cell activities F^O_i. The thalamic gate T_i (Eq. (43)) controlled by this loop remains closed until FEF plan layer cell activities F^P_i and LIP cell activities P^L_i contain consistent plans: active representations in FEF and LIP cooperate and compete with each other through reciprocal on-center off-surround projections that allow strongly activated plans to inhibit weaker plans until both areas contain representations that are consistent. Once the regions contain consistent saccade plans, they excite direct pathway cell activities B^D_i (Eq. (39)) which inhibit SNr cell activities B^N_i (Eq. (42)), releasing thalamic cells, with activity levels T_i, from inhibition. Once disinhibited, thalamic cell activity combines with FEF plan layer activity, allowing FEF output layer cell activities F^O_i to be excited. The FEF output layer then is ready to excite a corresponding saccade plan in further stages of the model, but cannot do so until a third BG gate is opened. Indirect pathway MSPN activities B^I_i (Eq. (40)) and GPe cell activities B^G_i (Eq. (41)) provide a constant source of inhibition to SNr cell activities B^N_i to ensure that only consistent FEF and LIP activity, resulting in strong direct pathway activity, is able to release thalamic activity T_i from inhibition.

The third gate controls outputs from the SC (Fig. 4(C)) and receives inputs from both FEF output layer cell activities F_i^O and LIP cell activities P_i^L, with special emphasis placed on the central region of the visual field where fixation cues are present, as in the WM loop. The presence of a fixation cue at the center of the visual field selectively activates the collicular loop indirect pathway MSPN activities G_i^I (Eq. (46)), which results in inhibition of GPe cell activities G_i^G (Eq. (47)), disinhibition of SNr cell activities G_i^N (Eq. (48)), and the consequent inhibition of colliculus cells with activities C_i (Eq. (32)). As long as a fixation cue is present, it is difficult for FEF or LIP to excite the activities G_i^D of direct pathway MSPNs (Eq. (44)) enough to overcome activity in the indirect pathway. If no fixation cue is present, and the saccade plans in FEF and LIP are consistent, this third gate opens, which allows FEF and LIP to excite SC cell activities C_i, leading to the production of the selected plan.

The three BG loops are critical for holding the model in a state of preparedness as information important for guiding its future responses is being presented, and detecting the task conditions which signal that it is time to utilize the stored information to drive behavior. This process depends largely on the presence and absence of the fixation point. When a fixation cue is present, the rehearsal and collicular gates are held shut and task-relevant cues are simply stored in memory. Once the fixation point is removed, SEF can select saccade targets from WM and excite corresponding representations in FEF. Provided the selected saccade plan is not inconsistent with any external cues represented in LIP, the FEF and collicular BG loops open their gates and allow plan signals to flow to SC, which generates the response.

2.6. Superior colliculus: saccade execution

The model SC contains a single population of cells, with activity levels C_i (Eq. (32)), which are excited by FEF output cell activities F_i^O and LIP cell activities P_i^L when saccade plan activities are sufficiently consistent to open the gate in the collicular loop (Figs. 1 and 4(C)). When SC cell activity C_i passes the saccade threshold ($\theta = 0.3$; Eq. (30)), the model's representation of eye position ε is updated, symbolizing the execution of a saccade. Suprathreshold SC activity excites FEF postsaccadic cell activities F_i^X responsible for inhibiting FEF plan and output layers (Fig. 1), clearing the plan from FEF, and preparing the system for the production of subsequent saccades.

2.7. Retinotopic and craniotopic coordinate frames

Two coordinate frames are used in the model: a *retinotopic* (eye-centered) frame is used in FEF (Bruce, Goldberg, Bushnell, & Stanton, 1985; Robinson & Fuchs, 1969; Saygin & Sereno, 2008) and SC (Sparks, Holland, & Guthrie, 1976; Wurtz & Goldberg, 1972), and a *craniotopic* (head-centered) frame is used in SEF (Bon & Lucchetti, 1990; Lee & Tehovnik, 1995; Schall, 1991; Sommer & Tehovnik, 1999) and PFC. Retinotopic representations change as the eyes move: Cues that excite the fovea are at the map's center while more eccentric cues are represented in the map's periphery. Retinotopic visual information is transformed into craniotopic representations by parietal *gain fields* (Andersen, Essick, & Siegel, 1987; Zipser & Andersen, 1988), which combine retinotopic data with eye position information, as in various regions of PPC (Saygin & Sereno, 2008; Zipser & Andersen, 1988).

Through gain fields, as in the ARTSCAN model (Fazl, Grossberg, & Mingolla, 2009), projections from PPC can excite targets that represent space in craniotopic coordinates via the map $W_{ij\varepsilon}^C$ (Eq. (4)). In our model, the primary target of PPC is PFC, which contains a craniotopic spatial WM (Fig. 1). Data support the idea that spatial WM in PFC uses a topographic representation of space, but experiments have been insufficient to determine whether that topography utilizes a craniotopic or retinotopic coordinate frame because monkeys have maintained fixation at a central cue as receptive fields have been mapped (Funahashi, Bruce, & Goldman-Rakic, 1989, 1990; Goldman-Rakic, 1996; Hagler & Sereno, 2006; Sawaguchi, 1996; Sawaguchi & Iba, 2001; Sawaguchi & Yamane, 1999). Our model uses a craniotopic coordinate frame in PFC because PFC interacts heavily with SEF, an area in which craniotopy has been repeatedly observed, and because such a representation is consistent with available data. That SEF uses a craniotopic representation has been demonstrated through microstimulation (Lee & Tehovnik, 1995) and electrophysiological studies (Isoda & Tanji, 2002, 2003; Lee & Tehovnik, 1995; Lu, Matsuzawa, & Hikosaka, 2002). Some have argued that the region also contains a retinotopic representation (Park, Schlag-Rey, & Schlag, 2006), others have suggested that SEF actually uses an object-centered representation (Olson & Gettner, 1999; Olson & Tremblay, 2000; Tremblay, Gettner, & Olson, 2002), while still others have shown that the coordinate system changes with learning (Chen & Wise, 1995a, 1995b, 1996; Mann, Thau, & Schiller, 1988). Despite these conflicting findings, the bulk of the data point toward a craniotopic SEF organization, and craniotopy is sufficient to support the model's operation and data simulations.

The model SEF excites selected saccade plans in FEF, which uses a retinotopic representation (Bon & Lucchetti, 1990; Lee & Tehovnik, 1995; Schall, 1991; Sommer & Tehovnik, 1999). Between SEF and FEF, cue representations are transformed back into a retinotopic coordinate frame, again using a gain field represented by $W_{ij\varepsilon}^R$ (Eq. (3)). This transformation requires eye position information, but because SEF is the recipient of a projection from PPC (Petrides & Pandya, 1984; Rizzolatti, Luppino, & Matelli, 1998), we hypothesize that it has access to eye position information which could facilitate the transformation. It is important that FEF uses a retinotopic frame because, in order to open BG gates, it must interact with PPC which, as mentioned above, uses a retinotopic representation that is modulated by gain fields. Finally, both PPC cells and FEF cells project to SC which also employs a retinotopic representation (Sparks et al., 1976; Wurtz & Goldberg, 1972).

Both representations are used because each confers distinct functional advantages, facilitating different processes. Regions that are involved with the production of eye movements, such as FEF and SC, use a retinotopic representation to direct saccades as a deviation from a current orbital position. Craniotopic representations, however, are particularly useful when representing a sequence of saccades (Grossberg & Kuperstein, 1989) because, even as the eyes move, the representation is stable throughout the entire process (Droulez & Berthoz, 1991; Mitchell & Zipser, 2003).

3. Results

3.1. Model simulations of basic oculomotor tasks

Our model builds upon the TELOS model of Brown et al. (2004) and the LIST PARSE model of Grossberg and Pearson (2008). The first simulations confirm that the current model can explain a set of basic oculomotor tasks that were summarized by Hikosaka, Sakamoto, and Usui (1989). These include the *saccade task*, *overlap task*, *gap task*, and *delayed saccade task* (Fig. 5). The ability to simulate these four tasks demonstrates that the model can saccade reactively toward cues (saccade task; Fig. 6), withhold saccades until task conditions permit their execution (overlap task; Fig. 7), and remember single saccade plans over a delay interval (delayed saccade task; Fig. 8). Model traces during each of these tasks are shown in Figs. 6–9.

In each simulation, the appearance of the fixation point leads to activation of cells in PPC areas 7*a* and LIP. Fixation-related activity

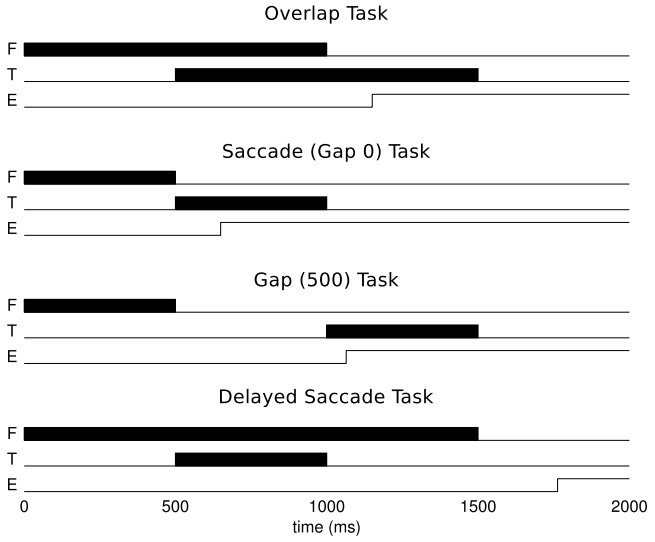

Fig. 5. Performance on benchmark saccade tasks. The model solves four benchmark oculomotor tasks: the saccade task, gap task, overlap task, and memory-guided saccade task. Saccade latencies in the four tasks are consistent with those observed in the literature. In particular, the model reproduces the gap effect by generating saccades at a much lower latency during the gap 500 task (64 ms) than during the saccade (gap 0; 137 ms) and overlap tasks (137 ms). Furthermore, saccade latencies are dramatically increased on the memory guided saccade task (256 ms). These latencies of the model are measured by the timing of its SC burst.

in LIP then excites direct pathway MSPNs in the collicular loop of the BG which inhibit colliculus-projecting SNr cells, rendering SC responsive to LIP activity, and leading to a saccade toward the fixation cue (Fig. 4(C)). In each of the oculomotor tasks in Fig. 4, a target is presented to which a saccade must be generated. If the fixation cue is still present when the target appears (overlap and delayed saccade tasks) then reactive saccades to the target are withheld because fixation-related activity in LIP activates the collicular loop's indirect pathway, holding SC under strong inhibition. In the overlap task (Fig. 7), where the target is still visible at fixation offset, LIP activity drives a saccade to the target once fixation is no longer required. In the delayed saccade task (Fig. 8), the target location must be stored in working memory. Fixation offset leads to the opening of the WM loop's rehearsal gate (Fig. 4(A)), allowing SEF to select the plan from working memory and excite a corresponding representation in FEF, which then excites SC to generate the saccade. In the saccade (gap 0; Fig. 6) and gap 500 (Fig. 9) tasks, the fixation point is removed as, or before, the target is presented. In these tasks, the model can saccade reactively to the target.

In addition to simulating each of these tasks, the model also produces saccades with the appropriate rank ordering of response latencies (Fig. 5). Most important among these latency effects is the *gap effect* (Fig. 9) which is characterized by short-latency saccades when the fixation point is removed in advance of the appearance of the saccade target (Jin & Reeves, 2009; Pratt, Bekkering, Abrams, & Adam, 1999; Saslow, 1967). Because the fixation point, presented at the beginning of each of these tasks, activates indirect pathway cells in the collicular BG loop, saccades cannot occur in response to other stimuli until activity in the indirect pathway, which strongly inhibits SC, subsides and the gate can open. When the fixation point is removed before the saccade target appears, activity in the indirect BG pathway subsides by the time FEF and PPC place bids to open the gate. Thus, advance removal of the fixation point allows the system to produce a saccade with a much shorter latency.

In addition to reproducing the gap effect, the model also takes longer to produce memory-guided saccades (Figs. 5 and 8), since additional BG gates need to be opened for the remembered saccade plans to be selected from WM by SEF, excited in FEF, and finally activate SC. Indeed, memory-guided saccades occur with longer latency compared to gap and overlap saccades (Gaymard, Ploner, Rivaud-Pechoux, & Pierrot-Deseilligny, 1999; Ozyurt, Rutschmann, & Greenlee, 2006), and functional magnetic resonance imaging data comparing performance on visually- and memory-guided saccades show that FEF, PPC and PFC are more strongly activated during memory-guided saccade tasks (Ozyurt et al., 2006), providing further support for the model.

3.2. Model simulations of the immediate serial recall task

To investigate the competencies of the Item-Order-Rank WM, the model was tested on the immediate serial recall (ISR) task which has served as a benchmark for models of sequential WM for many years. The ISR task can be divided into two phases. First, a sequence of cues is presented which must be remembered in order. Second, the cues are reproduced in the order in which they were presented. In our simulations, we first present a fixation cue toward which the model must execute a saccade. Then, a sequence of cues is presented at various spatial positions as fixation is maintained. Finally, the fixation cue is removed. Its disappearance acts as a 'GO' signal to saccade to each of the cued positions in order.

Fig. 10 shows relevant portions of the model throughout several critical points as the ISR task is executed. When the fixation cue is presented, it first excites the model parietal area 7*a* within which cell activities P_i^X, P_i^I, and P_i^Y generate a transient signal of cue onset that excites LIP cell activities P_i^L, but not WM cell activities M_{ir}. Because fixation cues are relevant to task success only when visible, representations of fixation cues are not instated into WM. Fixation-related information was excluded through a set of weights between model areas 7*a* and PFC (Fig. 10(C)). The representation of the cue in LIP cell activities P_i^L excites direct pathway MSPN activities G_i^D in the collicular BG loop which gates the excitation of SC cell activities C_i. Because no competing plans exist in FEF or LIP, the collicular loop quickly detects that a consistent saccade plan is prepared to activate SC and opens the gate, allowing information to flow from LIP into SC, which drives a saccade toward the fixation point (Fig. 10(A)). After this initial saccade has been executed, the fixation cue occupies the center of the PPC retinotopic gain field representation. Fixation cues excite indirect pathway MSPNs in the collicular BG loop, which results in strong inhibition of SC, prohibiting the production of future saccades (Fig. 10(B)).

As the model fixates on the central cue, a sequence of spatial targets is presented. Each of these cues, like the fixation point, excites PPC 7*a* cell activities P_i^X and P_i^Y (Fig. 10(C)). As each is presented, the population of SPL counting cell activities P_r^C is updated to reflect cue ranks: The SPL cell with the preferred rank of 1 is activated by the first cue, then cell 2 by the second cue, and so on. Information encoded by area 7*a* cell activities P_i^Y, which represent the spatial position of cues, and SPL cell activities P_r^C, that represent the ordinal position of cues, combines to excite position-rank cells in the PFC WM which receives convergent projections from 7*a* and SPL (recall Fig. 2). The rank-selective spatial cue representations so instated into WM form an activity gradient over WM cell activities M_{ir}. As long as the fixation point remains visible, the model stays in this state of preparedness. No information flows from WM to SEF because LIP fixation activity holds closed the rehearsal gate R of the WM loop (Fig. 10(C)).

The moment the fixation point is removed, the rehearsal gate R opens, and WM cell activities M_{ir} begin exciting SEF cell activities S_{ir}^X (Fig. 10(D)). The winner-take-all network in SEF chooses the most active representation, which alone remains active in SEF as it inhibits all other representations. When the winning activity

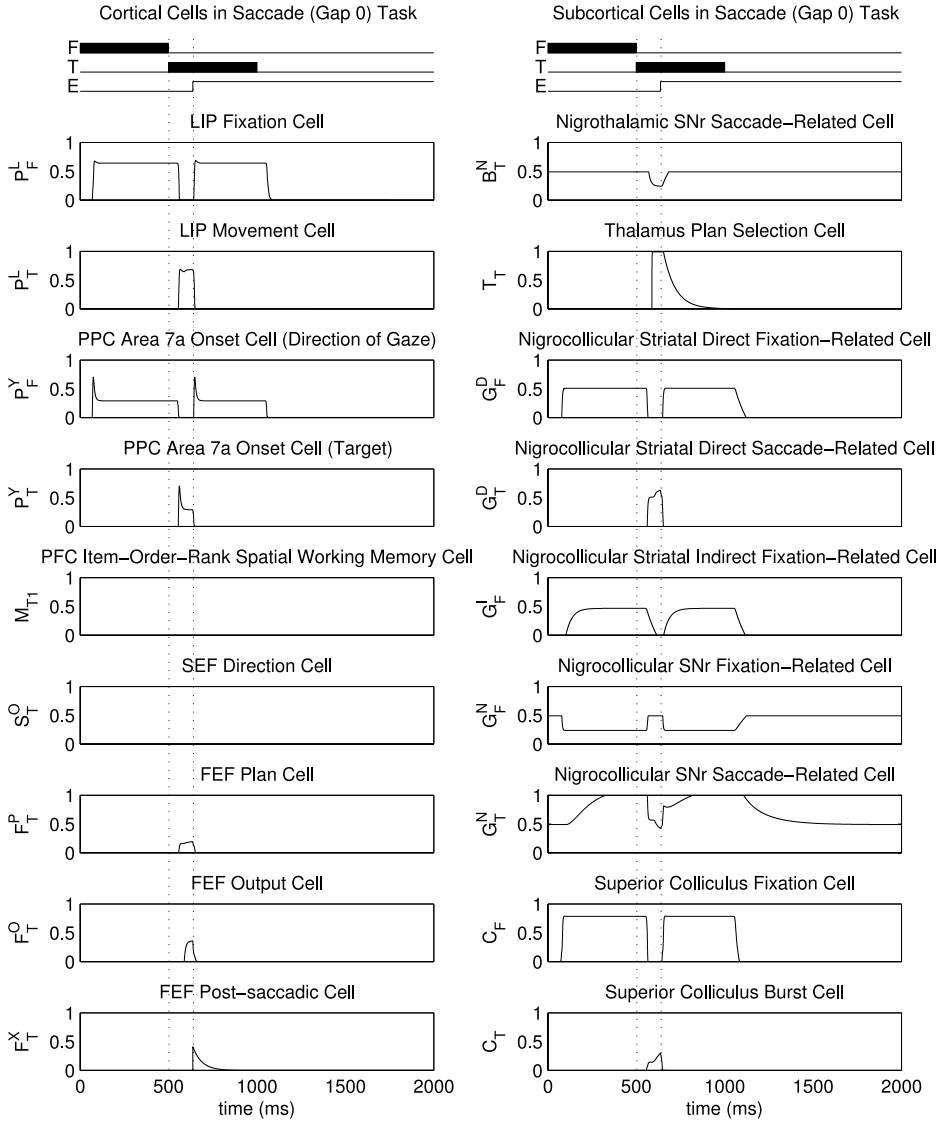

Fig. 6. Model cell traces during the saccade (gap 0) task. In this task, target onset and fixation offset are simultaneous. The model does not execute a saccade to the target until fixation-related SNr activity ceases, and the nigrocollicular gate is opened. *Left column*: cortical cell activities; *right column*: subcortical activities. Subscripts *F* and *T* denote activities of cells responsive to fixation and target, respectively.

exceeds a threshold, it activates SEF output layer cell activities S_i^O, which in turn activate FEF plan layer cell activities F_i^P (Fig. 10(E)). Simultaneously, a strong inhibitory signal feeds back from SEF cell activities S_{ir}^Y to WM cell activities M_{ir} and deletes the just-selected representation from WM.

FEF plan layer cell activities F_i^P seek to excite FEF output layer cell activities F_i^O but must first open the gate controlled by the FEF loop of the BG, which controls the flow of information from the FEF plan layer to the FEF output layer. Because, in this task, there are no longer any cues present in the environment, LIP does not contain any representations that are inconsistent with that which has just been excited in the FEF plan layer. As such, the gate opens and the plan is excited in the FEF output layer (Fig. 10(F)). Again, the plan sends bids to the BG, this time seeking to open the collicular gate which controls excitation of the SC cell activities C_i, and ultimately the production of the saccade. There are still no cues represented in LIP, and the fixation point is not present, so the gate quickly opens allowing FEF output layer cells to excite SC and produce a saccade (Fig. 10(F)).

While selected plan signals flow through FEF, open BG gates, and activate SC, the SEF is able to make its next selection. Again the representations in WM excite SEF selection cell activities S_{ir}^X and S_{ir}^Y (Fig. 10(D)), through which a competition is staged and the most active representation is chosen. Once a representation wins this competition, the plan is again excited in SEF output cell activities S_i^O and deleted from WM (Fig. 10(E)). The plan is instated into FEF cells and, still unchallenged due to the continuing absence of inconsistent cue representations in LIP, opens the two BG gates and excites SC cells to produce a saccade (Fig. 10(F)). This process continues until no plans remain in the WM, at which point SEF cells no longer receive their driving input from WM.

Fig. 11 shows cell traces from several model areas as the ISR task is solved with a sequence following the pattern A–B–A–C, which contains a repeat of the same spatial position (represented here with 'A') at the first and third ordinal positions. When the fixation point is presented at the beginning of the task, it excites the model PPC area 7*a* cell activities P_i^X and P_i^Y (Fig. 11(A)) which excite LIP cell activities P_i^L (Fig. 11(B)). An initial excitatory response can be seen in both of these fields in response to the fixation point. Because there are no plans in FEF, the LIP representation opens the collicular BG gate that controls excitation of SC. Gate opening is marked by a reduction in the colliculus-projecting SNr

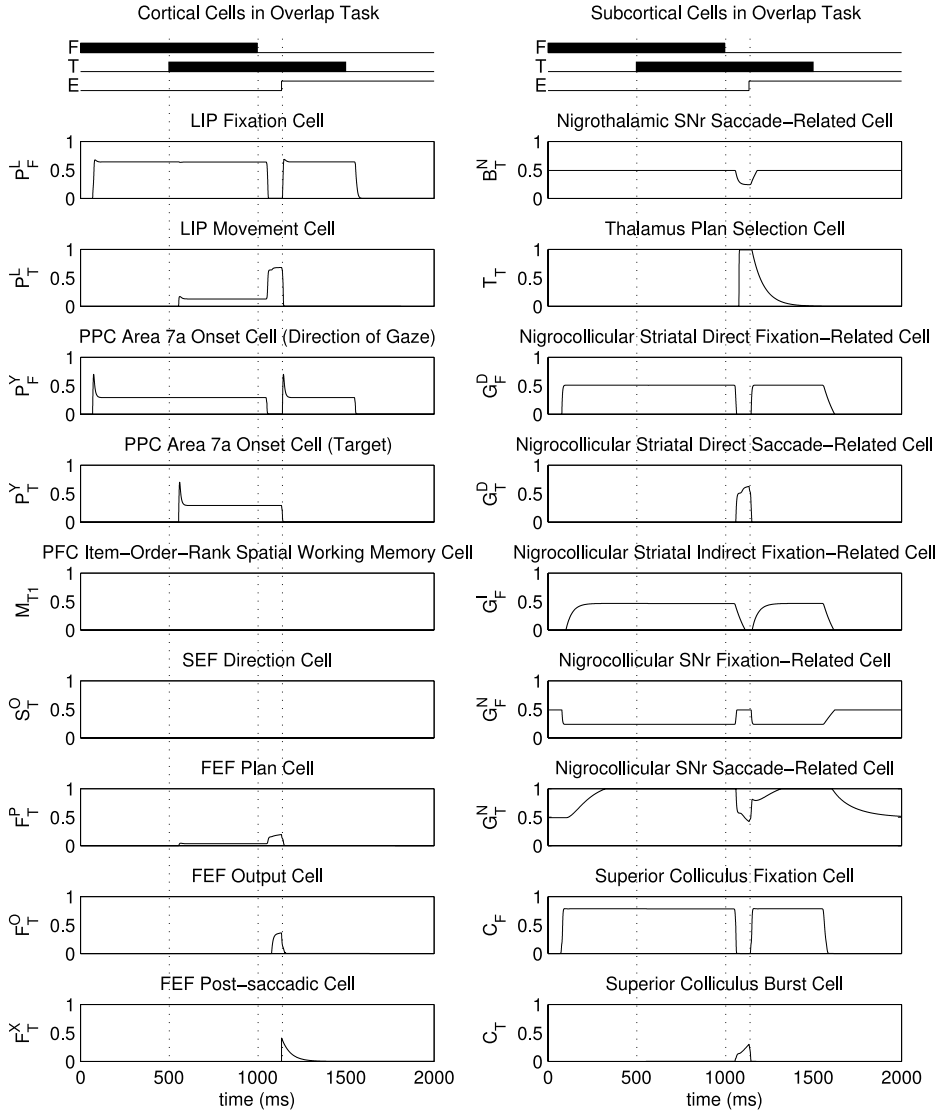

Fig. 7. Model cell traces during the overlap task. In the overlap task, the target appears before fixation offset. The model does not respond to the target until LIP fixation activity P_i^L subsides. Conventions as in Fig. 6.

cell activities G_i^N (Fig. 11(H)). Released from inhibition, SC cell activities C_i are excited (Fig. 11(I)) by the representation of the fixation point in LIP to initiate a saccade.

After the saccade occurs, the fixation point is foveated and excites the central spatial position in retinotopic coordinates. Because the fixation point has now changed its retinal position, PPC cells are excited once again, indicated by the second rising trace in 7*a* and LIP (Fig. 11(A) and (B)). As long as the fixation point remains visible, other LIP cells are inhibited and thus relatively unresponsive to subsequent cues. The strong and sustained fixation activity in LIP holds the BG gate closed, as can be seen by the increased SNr cell activity G_i^N (Fig. 11(H)) that corresponds to all spatial positions *other* than the center. For central representations the gate remains open allowing central SC cells to fire continuously throughout fixation (Fig. 11(I)). As the sequence of spatial cues is presented, 7*a* cell activities P_i^Y mark the cue onsets with transient peaks, and SPL counting cells reflect the rank of each cue (Fig. 11(C)), while LIP cell activities P_i^L are only weakly activated. The 7*a* cells excite WM cell activities M_{ir} (Fig. 11(D)) that store rank-sensitive cue representations in an activation gradient similar to that observed by Averbeck et al. (2002).

The rehearsal period, during which saccades are executed to the cued positions in order, is marked by the removal of the fixation point (dotted line, Fig. 11). The first response to fixation offset in the model is the decay of fixation-related activity in PPC areas 7*a* and LIP (Fig. 11(A) and (B)) as well as in SC (Fig. 11(I)). Simultaneously, colliculus projecting SNr cells (Fig. 11(H)) move toward their baseline level of activation. Once the representation of the fixation point in LIP is weak enough, the BG WM loop's rehearsal gate R opens, allowing PFC cell activities M_{ir} to excite SEF cell activities S_{ir}^X and S_{ir}^Y (Fig. 11(E)). Initially, each WM trace excites a corresponding cell in SEF, visible as the several simultaneously rising traces on the leading edge of the first peak in SEF cell activities S_{ir}^Y. The strongest WM representation, however, provides the strongest drive and the associated SEF cells win the competition, ultimately inhibiting other SEF cells, whose activities drop. Once SEF selection cells pass a threshold, they delete the selected representation from WM, shown in Fig. 11(D) as a rapid decrease in activation of the strongest WM trace. Simultaneously, SEF output cell activities S_i^O (Fig. 11(F)) are excited, thereby introducing the selected plan into FEF. The responses of FEF output cell activities F_i^O (Fig. 11(G)) display the characteristic phasic responses of FEF presaccadic cells (Bruce & Goldberg, 1985), with responses of a shorter duration than those in SEF (Hanes, Thompson, & Schall, 1995; Isoda & Tanji, 2003), and ultimately open the collicular BG gate (Fig. 11(H)) which removes SC cell

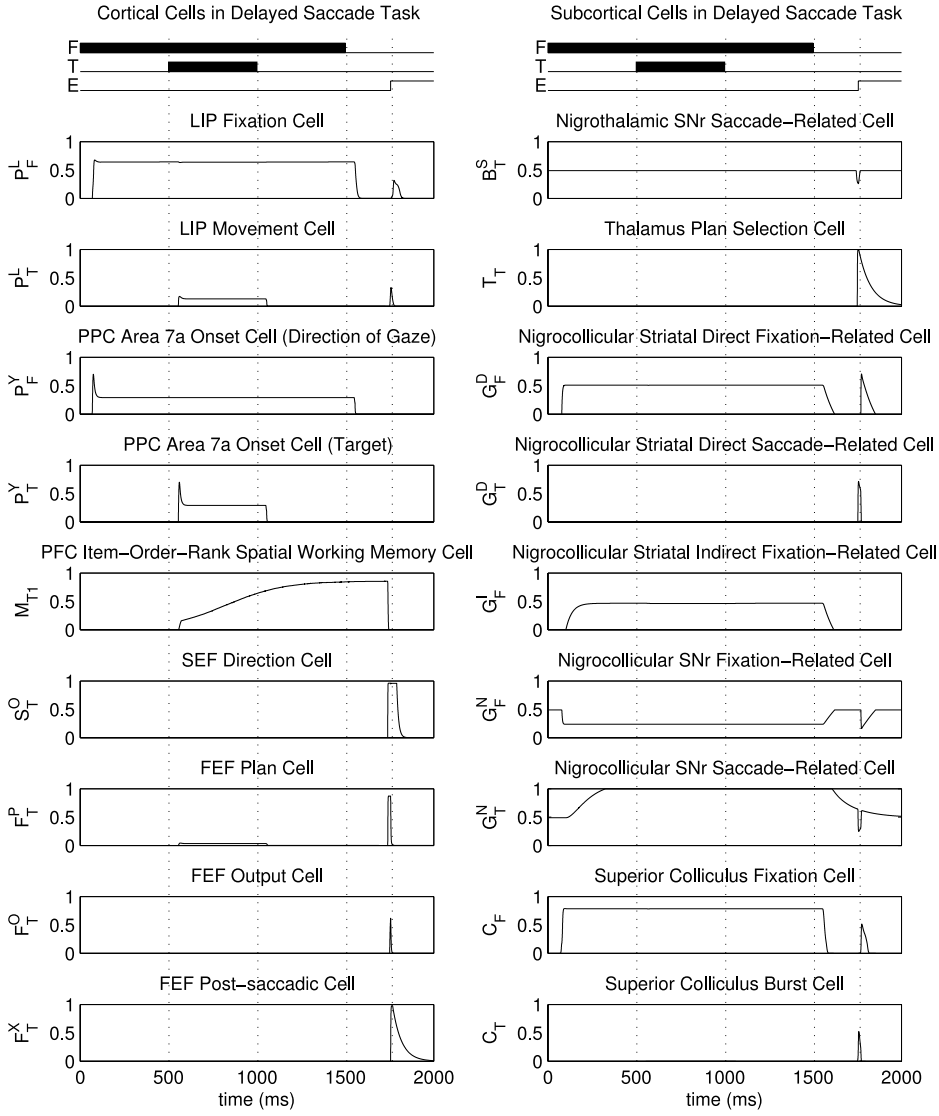

Fig. 8. Model cell traces during the delayed saccade task. In the delayed saccade task, the target is presented during fixation. After fixation offset, a saccade is generated to the remembered location. This task requires SEF to select the remembered plan from working memory. Conventions as in Fig. 6.

activities C_i from inhibition (Fig. 11(I)) so they can burst, generating saccades.

LIP, FEF, SNr, and SC activities (Fig. 11(B), (G)–(I), respectively) are characterized by double-peaks as saccades are produced. The second peak occurs because these areas represent space in retinotopic coordinates. Following saccades, SEF activity continues to excite FEF cells. Because the eyes have moved, the map $W^R_{ij\varepsilon}$ that transforms representations from craniotopic to retinotopic coordinates leads to excitation of the saccade target's new retinotopic position: the center of the visual field. Peaks appear in LIP as saccades are produced because FEF and LIP are characterized by a cooperative–competitive interaction, and FEF excites LIP cells in order to produce a state of coherence between the two fields, required to open the nigrocollicular gate and produce a saccade. Double peaks in FEF are therefore transferred to LIP. In each of these areas, the second peaks represent the just-completed saccade plan in a new frame of reference.

3.3. Microstimulation in saccade tasks

The model also reproduces behavioral results that have been observed during SEF microstimulation. Histed and Miller (2006) trained monkeys to perform a task in which two spatial positions were sequentially cued during an initial fixation phase, remembered during a memory delay, and then visited in order with a sequence of saccades following the offset of the fixation point. On each trial, two adjacent spatial cues were chosen from among six possible cue positions. The first cue was presented after fixation had been maintained on the fixation point for 500 ms, and the second cue was presented after a variable delay, or stimulus (cue) onset asynchrony (SOA), which ranged from 0 to 200 ms. Trials with large SOAs were easiest for trained monkeys to solve, approaching ceiling performance levels, whereas trials in which cues were presented simultaneously (SOA $=$ 0 ms) were characterized by chance performance. Finally, on some trials, microstimulation was applied to SEF for the first 900 ms of the 1000 ms WM delay interval, prior to the offset of fixation.

Remarkably, such stimulation did not disrupt the monkey's ability to correctly saccade to the remembered target locations. But it did disrupt the order of saccades. For each microstimulation site, ordering performance was evaluated within each of the six pairs of targets as a function of SOA, where "positive SOAs indicate that the more ipsilateral target appeared first, and negative SOAs, the more contralateral target first" (Histed & Miller, 2006). Fig. 12(A) shows three plots, each corresponding to a single pair of cues and a microstimulation site, showing the fraction of trials in which

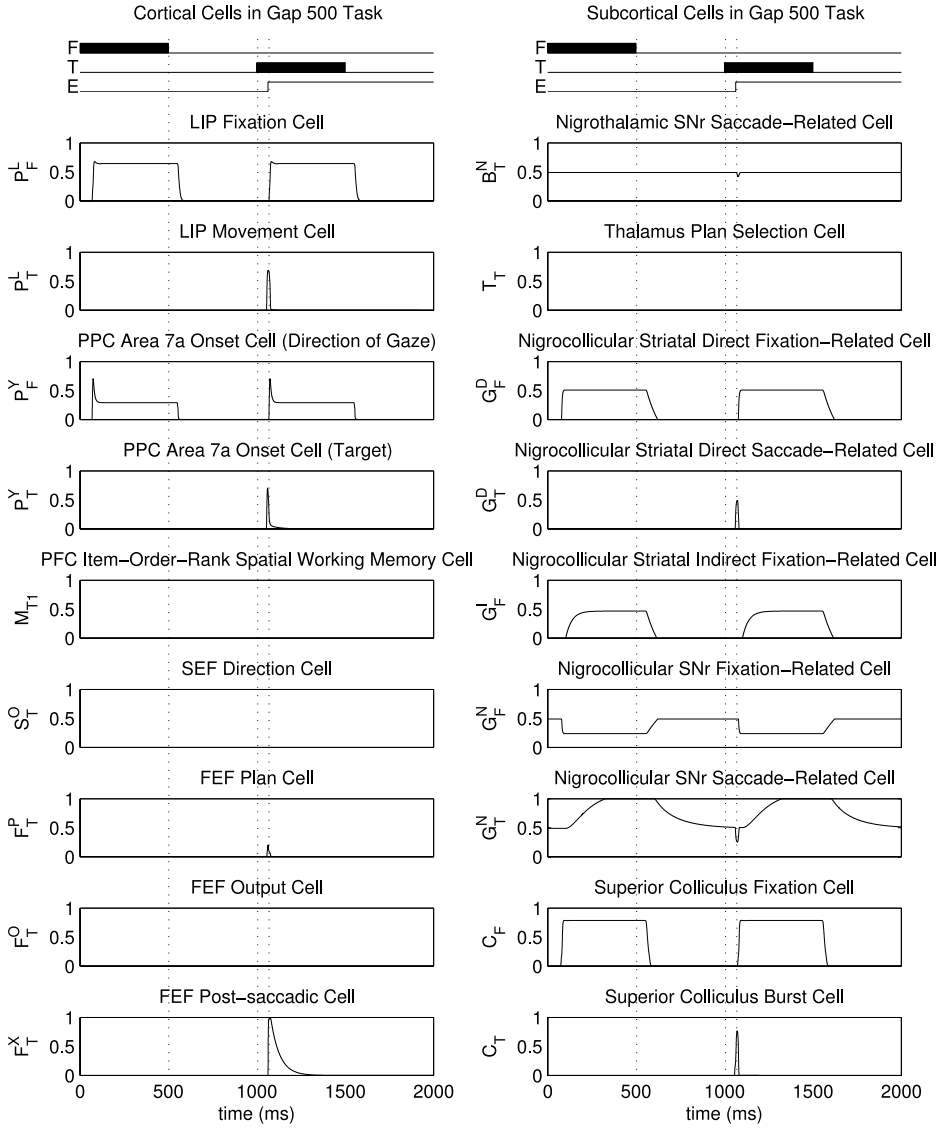

Fig. 9. Model cell traces during the gap (gap 500) task. In the gap task, fixation offset occurs in advance of target presentation. Fixation-related SNr activity has ceased by the time the target is presented, leading to shorter latency saccades. FEF plan layer cells respond weakly, while FEF output cells remain quiescent, because the model reactively saccades to the cue so rapidly that there is insufficient time for activity to build. Conventions as in Fig. 6.

the first saccade was directed toward the more ipsilateral target first. For large-magnitude SOAs, response orders are typically correct. As SOA decreases, initial responses are increasingly mixed, and when targets are presented simultaneously (SOA = 0 ms) monkeys perform at chance, saccading to either target first with equal probability. Probabilities from both unstimulated (black) and stimulated (gray) trials were fit with logistic regression curves that estimate the likelihood of an initial response to the more ipsilateral target for a given SOA.

That microstimulation biased the order in which saccades occurred is shown by the leftward shift of the microstimulation (gray) curves. On microstimulation trials in which the cues are presented simultaneously (SOA = 0 ms), monkeys are more likely to saccade to the target that is more ipsilateral, with respect to the hemisphere in which microstimulation is applied, as their first response. In some cases, initial responses are directed toward the more ipsilateral target for nearly all SOAs following microstimulation (Fig. 12(A), upper left). Model simulations of microstimulation trials reproduce this phenomenon (Fig. 12(B)), causing curves (gray) to shift by magnitudes that approximate the experimental shifts. Each plot in Fig. 12 depicts the effect of microstimulation at a different site. In simulations, the magnitude of the shift is proportional to the distance between the stimulating electrode and cortical representations of saccade targets.

In the model, long duration microstimulation causes habituation in SEF synapses between rank-direction cells with activities S^X_{ir} and S^Y_{ir}. Habituation is strongest in synapses of cells close to the microstimulation site, reducing their efficacy in subsequent task intervals. During the selection process, when saccade targets are chosen from WM on the basis of their activation strengths, weakened synapses result in a reduced likelihood of selection. SEF cells close to the microstimulation site are therefore less able to influence the competition, giving more distant cells an advantage. Fig. 13 shows model activity during a control trial (left) and during a trial in which microstimulation is applied (right). Microstimulation-induced habituation, shown by decreasing strength in habituative gates, occurs during the stimulation interval, and then remains for some time after the offset of microstimulation. The right column of Fig. 13 shows a trial in which microstimulation led to the selection of the weaker WM representation, thereby reordering the saccade sequence.

Because the model attributes the microstimulation-induced breakdown of saccade ordering to SEF habituation, and not to

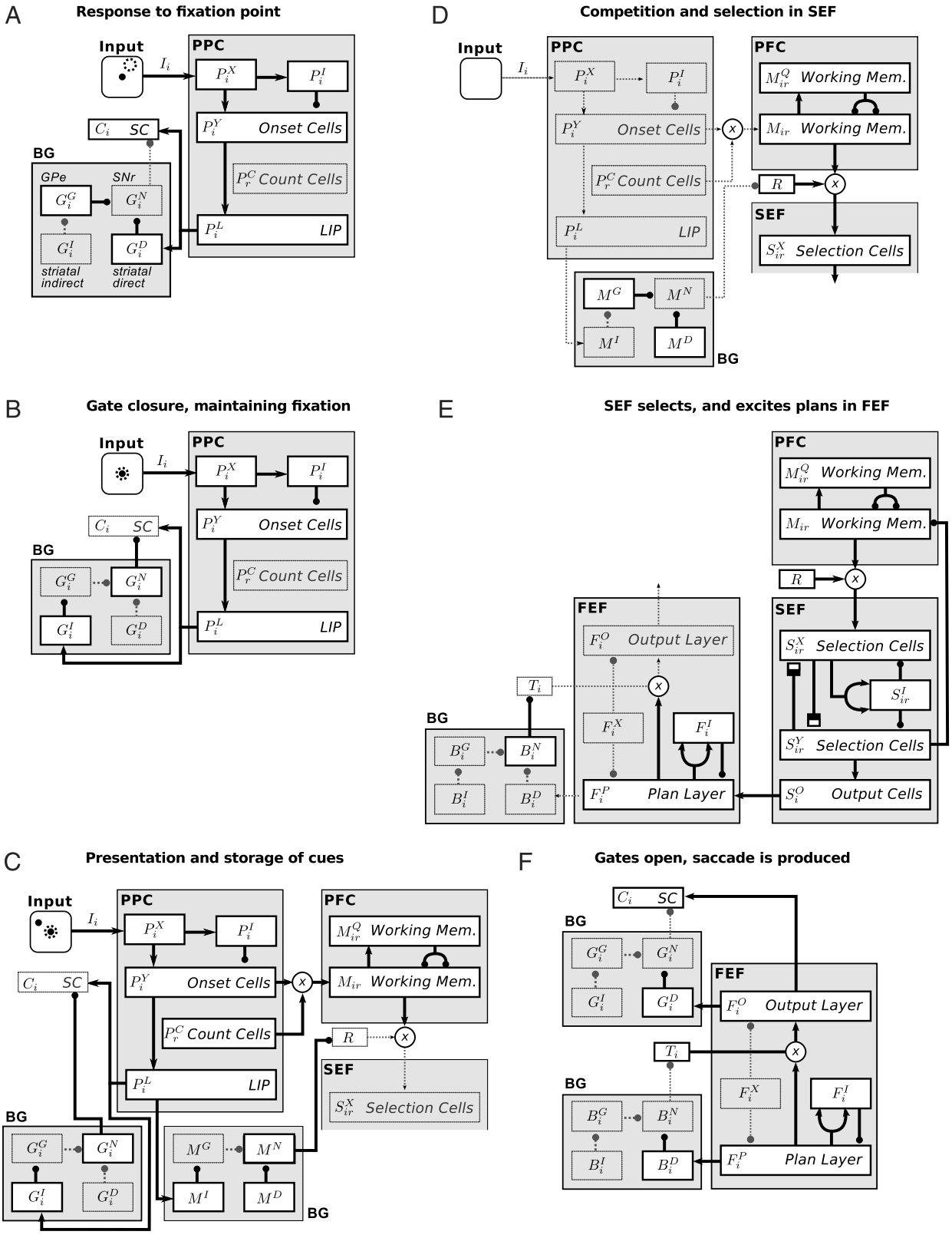

Fig. 10. Model stages during the ISR task. Each panel depicts portions of the model relevant for a particular process as the model solves the ISR task. Gray fields are those that are effectively removed from the system by either inhibition or lack of excitation. White, bold stroke fields are active, and participate in the process being explained in each panel. The dotted circle in the input space of panels A–C represents the direction of gaze. (A) The model saccades to the fixation point. Anatomical labels shown in this panel for BG apply to all panels. (B) Fixation is maintained. (C) A sequence of spatial cues is presented and stored. Neither saccades nor selection can occur because gates are held closed by fixation-related LIP activity. (D) Fixation point removal opens the rehearsal gate *R* via the BG working memory loop (Fig. 4(A)), and allows selection to begin in SEF (cf. Grossberg & Pearson, 2008). (E) Selected saccade plans are excited in FEF and deleted from working memory. (F) FEF and collicular gates open, allowing the saccade plan to flow through FEF and to SC, which generates a saccade. Operations in panels D–F repeat until no representations remain in the working memory.

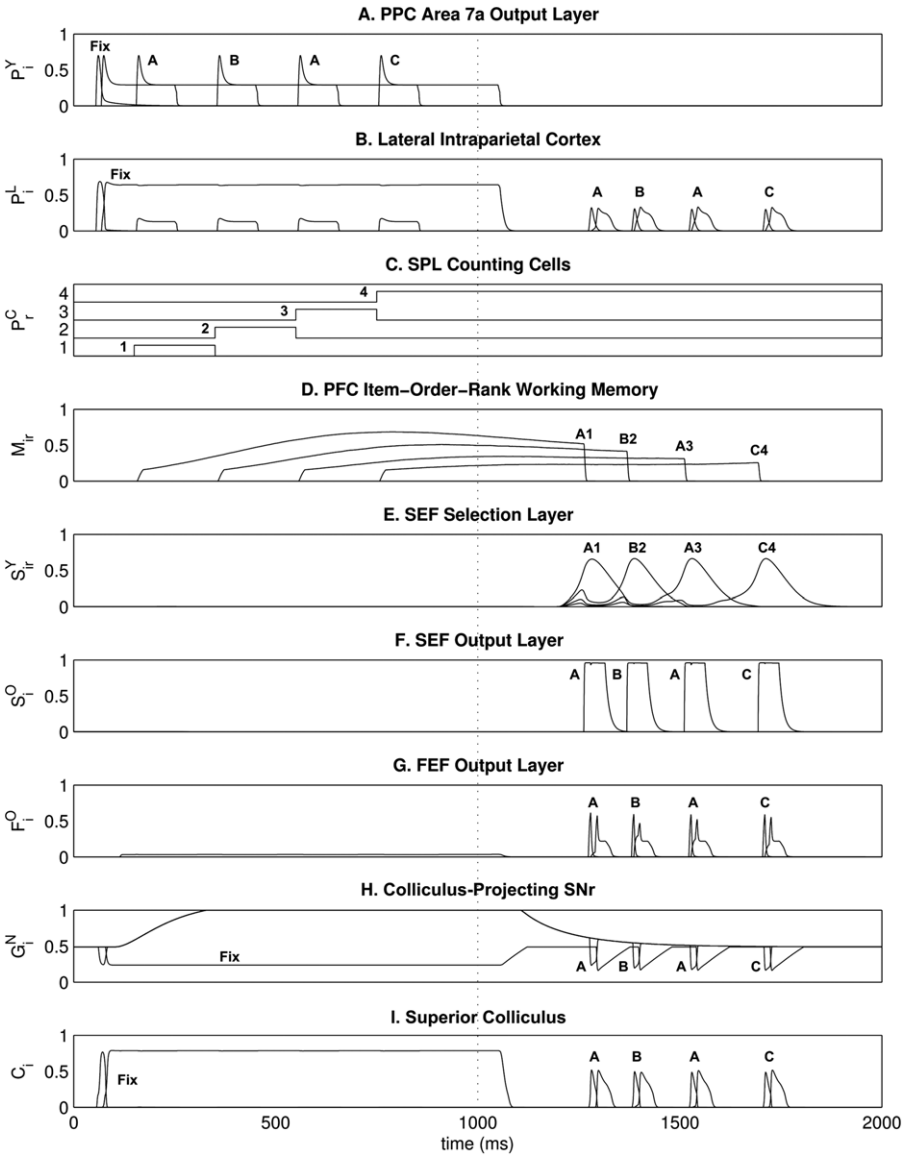

Fig. 11. Activity traces from selected cells as the model solves the ISR task. In the first half of the task, the model simply stores representations of all of the cues that are presented (other than the fixation point). Transient responses to onsets are visible in cell activities P_i^Y, and are held well below threshold, by fixation related activity, in LIP cell activities P_i^L. Working memory cell activities M_{ir} can be seen building up following each presentation, and preserving the order in which cues are presented. Once the fixation point is removed, a sequence of saccades is produced to the cued positions. While the sequence is produced, the responses of SEF selection cell activities S_{ir}^Y, output cell activities S_i^O, FEF output cell activities F_i^O, collicular-projecting SNr cell activities G_i^N, and SC cell activities C_i for each saccade are visible. The selection of the appropriate saccade target occurs initially in SEF, which also deletes the selected representation from working memory traces, and then excites the remaining fields in order to produce the saccade.

loss of order information from WM, it predicts that a *longer delay* between microstimulation offset and fixation cue offset (the "recall now" cue) could actually improve saccade ordering, if the delay is long enough to allow recovery of the habituated SEF synapses. By the end of trials the degree of habituation is significantly attenuated (Fig. 13) which allows selection to occur normally.

Histed and Miller (2006) also considered the way microstimulation at a single site biases responses at all cue pairs collectively (Fig. 14(A)). They observed that the strength of the bias varied across the different cue pairs (insets), with the microstimulation-induced saccade trajectories (arrows) following a pattern in which final saccades were directed toward a *convergence zone*, an effect that is also reproduced by simulations (Fig. 14(B)). Fig. 14(C) shows the microstimulation-induced trajectories on top of the two-dimensional Gaussian kernel used to represent microstimulation in model simulations (Section 4.8, Eq. (26)). The center of the Gaussian represents the microstimulation site, and is located at the approximate position of the convergence zone. The microstimulation-induced trajectories appear to 'climb' the Gaussian; in all cases, the target farthest from the microstimulation site is least affected by microstimulation and therefore more likely to win the competition and serve as the first saccade target. The second saccade is directed toward the remaining target, which is closer to the center of the Gaussian, producing the climbing trajectories and convergence effect.

Another important finding of Histed and Miller (2006) was that microstimulation had no effect on saccade accuracy, peak velocity, or latency. These observations suggest that SEF is not involved in the storage, generation, or fine timing of saccades. A target selection system is consistent with these data because SEF microstimulation manipulates only the potency with which plans compete and, during fixation while BG gates are closed, do

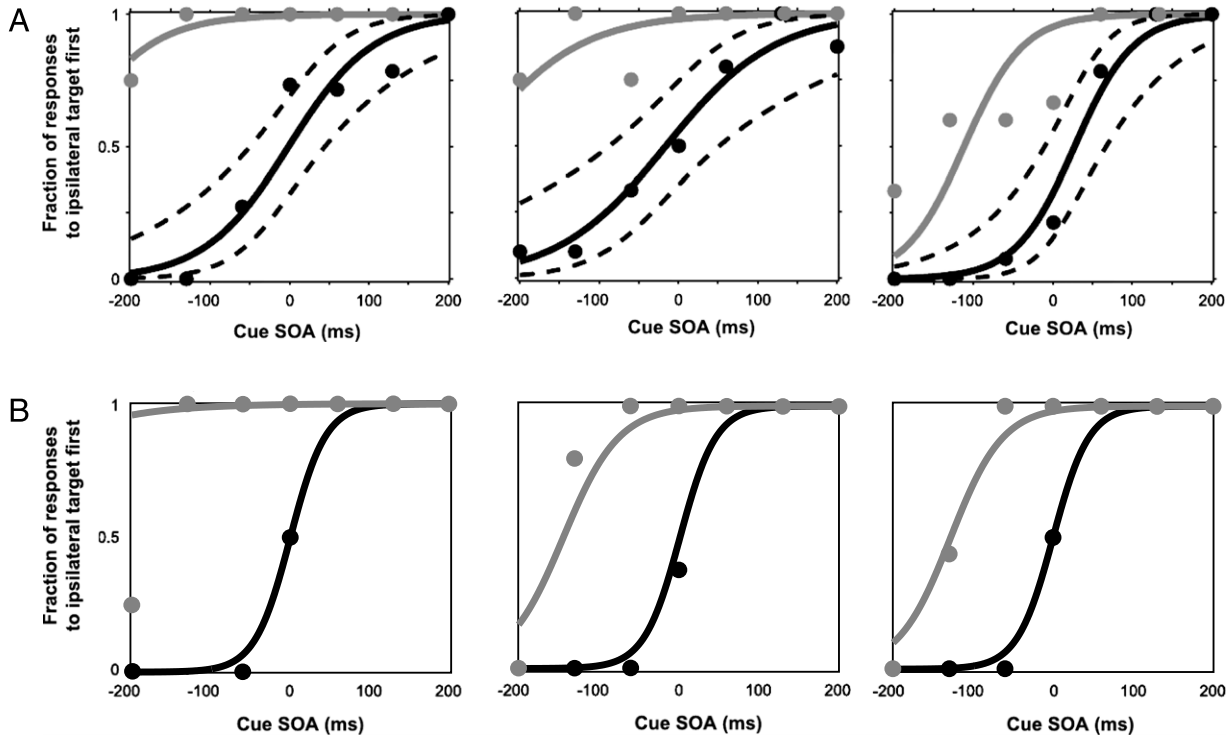

Fig. 12. SEF microstimulation can reorder a remembered spatial sequence. (A) Data from three microstimulation sites showing that microstimulation (gray) in SEF biases saccades compared to controls (black) so that the more ipsilateral target, with respect to the hemisphere in which microstimulation is applied, is more likely to be visited first. (B) Model results.
Source: Data adapted with permission from Histed and Miller (2006).

not generate new saccade targets. Moreover, if SEF selects targets but does not issue the motor commands that move the eyes, saccade velocity remains unchanged. So long as the duration of the selection process is not changed by microstimulation, saccade latency will also remain unchanged, as demonstrated by the simulated latency distributions in Fig. 15(B).

Another study with SEF microstimulation, however, shows that microstimulation *can* change saccade latency. Yang et al. (2008) required monkeys to solve a simple saccade (gap 0) task in which fixation had to be maintained at a central cue for 500 ms, after which a target would appear at a position to either the left or right of fixation. Monkeys would then saccade to the target, and fixate there until the end of the trial. On some trials, microstimulation was applied throughout one of two 100 ms intervals: an early interval beginning 25 ms before the appearance of the saccade target, and a late interval beginning 75 ms after the appearance of the saccade target, which coincides with the approximate mean visual response latency of SEF and FEF (Goldberg & Bushnell, 1981). Their data show that microstimulation in these two intervals can reduce and increase saccade latency (Fig. 16(A)–(C)), a finding superficially inconsistent with the Histed and Miller (2006) finding that microstimulation did not change latency.

Our model can reproduce these data as well (Fig. 16(D)–(F)). The latency change arises because of the temporal proximity of microstimulation to the offset of fixation, and therefore the beginning of the response interval. Whereas microstimulation applied by Histed and Miller (2006) ended 100 ms before the offset of fixation, SEF microstimulation in the Yang et al. (2008) task occurs only 25 ms before or 75 ms after cue onset. The injection of current caused by SEF microstimulation influences FEF activity as saccade commands are being processed by these areas. When this FEF excitation is consistent with FEF saccade plans, it strengthens plan representations, thereby accelerating gate opening and facilitating saccade production. If, however, microstimulation-induced excitation of FEF cells is *inconsistent* with the saccade being planned, local inhibitory interactions in FEF slow the planning process because plans compete. Once a single, strong saccade plan emerges, it opens the BG gate, producing a saccade with increased latency. In simulations of this task, FEF saccade plans only become strong enough after such inconsistent microstimulation has ceased. Our simulations show how microstimulation that occurs as saccades are being planned, as in the Yang et al. (2008) task, can interfere either constructively or destructively with those plans leading to facilitation or delay of saccades, respectively. The model explains how microstimulation, when applied at different sites, during different task intervals, and for different durations, can sometimes change latency and sometimes not.

3.4. Temporal dynamics of multiple cell types

Model cells behave like electrophysiologically identified cell types. Fig. 17(A) pairs model transient onset PPC cells with corresponding data showing PPC cells that behave similarly. In order for cues to be instated into WM, cue presentations are detected by transient onset cell activities P_i^Y, observed in PPC (Bisley, Krishna, & Goldberg, 2004), which fire strongly at the presentation of visual stimuli and then reduce their firing rate while the cue remains on. Also modeled are LIP movement cell activities P_i^L (Andersen et al., 1987; Brown et al., 2004; Colby, Duhamel, & Goldberg, 1996), which are important for driving saccades and participating in the model gating process (Fig. 17(B)).

Fig. 17(C) depicts SEF rank-direction cell activities S_{ir}^X (Isoda & Tanji, 2002, 2003). Isoda and Tanji (2002) and Lu et al. (2002) also observed direction cells, represented by SEF output cell activities S_i^O (not shown), and rank cells. Although our model does not

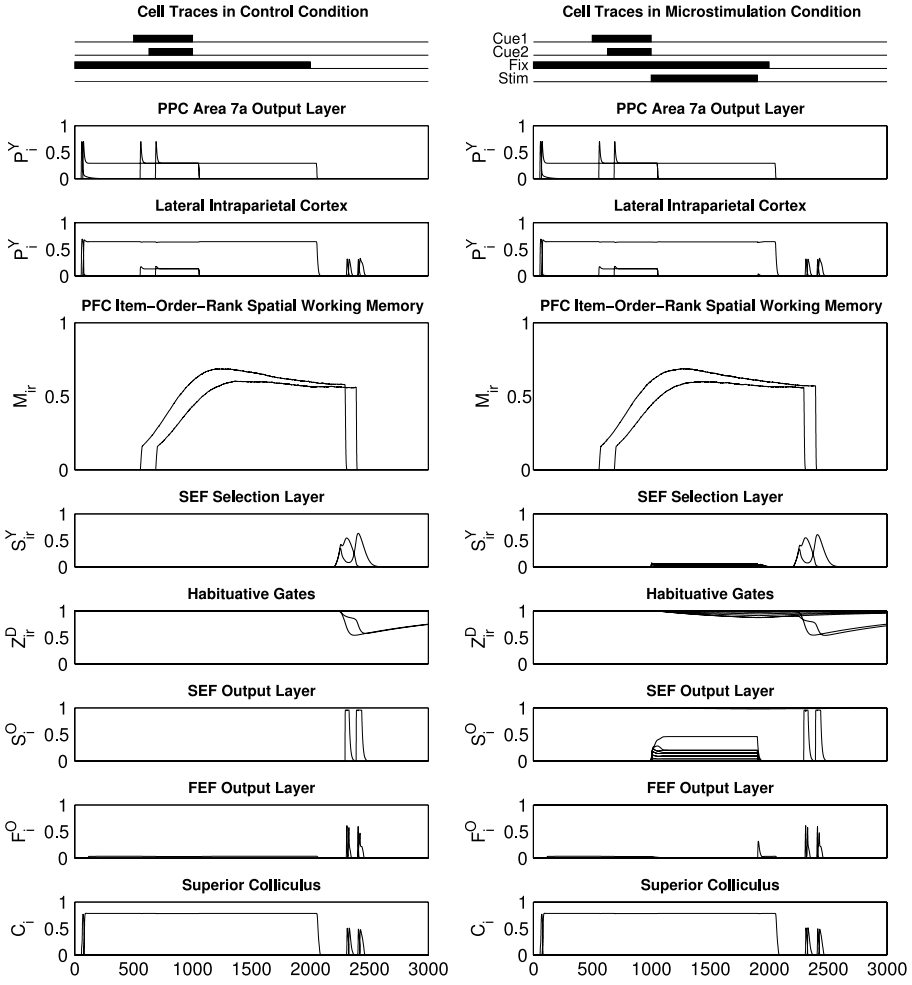

Fig. 13. Cell traces in Histed and Miller (2006) task. During control trials (*left column*), cued locations are stored and recalled as in the ISR task. When microstimulation is applied, SEF cells are activated and habituative gates depleted. Habituation can cause the weaker working memory representation to be selected first, reordering the sequence. Microstimulation produces stronger excitation in SEF output cell activities S^O_{ir}, compared to selection cell activities S^X_{ir} and S^Y_{ir}, because they are not in a competitive network, and therefore not recipients of recurrent inhibition. Microstimulation produces a small burst in FEF cells, but the presence of fixation activity in LIP ensures that a saccade is not produced.

explicitly reproduce SEF rank cells, we hypothesize that the SEF rank-direction population comprises a continuum of cells, some of which are purely rank-selective, some purely direction-selective, and some with the rank-direction responses shown here.

Fig. 17(D) compares FEF presaccadic cell activity (Brown et al., 2004; Bruce & Goldberg, 1985; Hanes et al., 1995; Isoda & Tanji, 2003; Schall, 1991) with model FEF output cell activities F^O_i which excite SC cells, leading to saccade initiation. Presaccadic cells in the model can be found in both the FEF plan layers and output layers, although on some occasions plan cells can sometimes precede the execution of the saccade by a longer interval because task demands require that other actions need to be taken before FEF saccade commands can be executed. Fig. 17(E) compares postsaccadic cell recordings (Bizzi, 1968; Brown et al., 2004; Schall, 1991) with model postsaccadic cell activities F^X_i, which are activated by feedback from SC cells and are important for silencing excitatory FEF cells to prepare them for the processing of subsequent saccade commands.

Finally, the model reproduces several subcortical cell types (Fig. 17(F)–(H)). Most notable are SNr cell activities G^N_i that pause (Fig. 17(F); Brown et al., 2004; Hikosaka & Wurtz, 1989), releasing SC from inhibition and allowing cell activities C_i to burst (Brown et al., 2004; Munoz & Wurtz, 1995), thereby generating saccades (Fig. 17(G)). Also modeled are fixation cell activities C_i in SC (Brown et al., 2004; Munoz & Wurtz, 1993), which are active during maintenance of fixation and pause during saccades (Fig. 17(H)).

4. Mathematical model

4.1. Implementation and shunting equations

The model was implemented as a system of ordinary differential equations, and simulated in MATLAB using a fourth order Runge–Kutta numerical integration method. Fig. 1 shows all of the model cell types accompanied by the variables which represent their membrane potentials, as described by nonlinear membrane, or shunting, equations (Grossberg, 1968, 1973; Hodgkin, 1964). Shunting equations follow the general form

$$\frac{dx_i}{dt} = -Ax_i + (B - x_i)I^E_i - x_i I^I_i, \tag{1}$$

where x_i represents the activity of a cell; the parameter A represents the rate of passive decay, which controls how fast the cell returns to its baseline level of activation in the absence of inputs; parameter B is the excitatory saturation constant, which represents the maximum value of x_i; and I^E_i and I^I_i are expressions containing all excitatory and inhibitory inputs, respectively.

4.2. Visual inputs

At each time step, the visual field is divided into a two-dimensional 9 × 9 grid centered over the input space. If a cue is

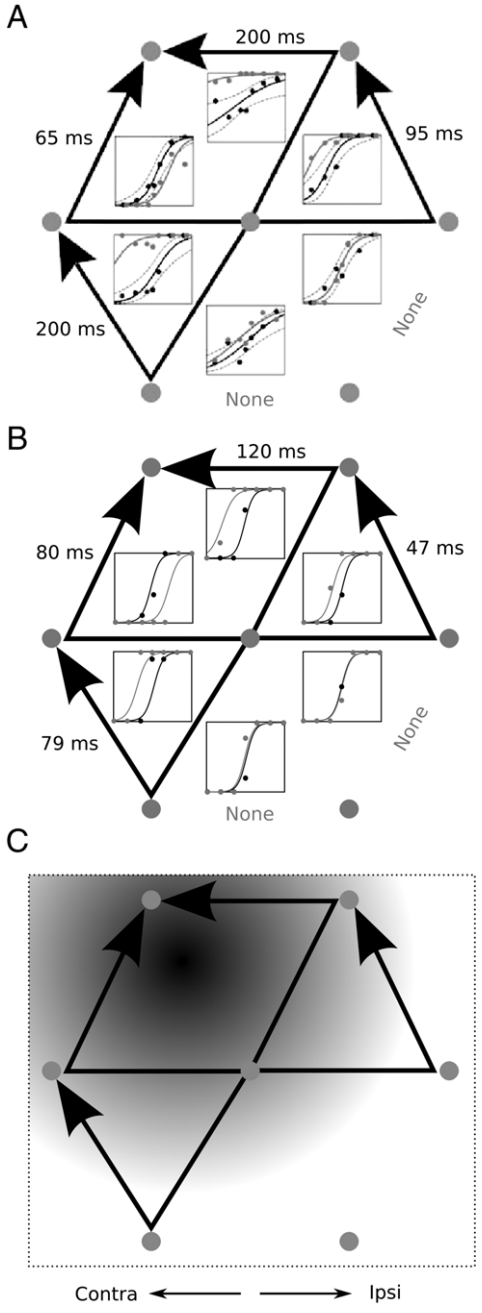

Fig. 14. SEF microstimulation causes saccade trajectories to converge. The bias observed for each of the six pairs of adjacent cues (insets) can be used to identify the saccade trajectory rendered more likely by microstimulation (arrows). (A) Observed saccade trajectories that converge toward the upper left target. (B) Model simulations reproduce the convergence effect. (C) In model simulations, microstimulation habituates synapses according to a two-dimensional Gaussian function centered over the microstimulation site. Saccade trajectories following microstimulation tend to 'climb' the gradient.
Source: Data adapted with permission from Histed and Miller (2006).

present at any of the $i \in [1, \ldots, 81]$ positions, representing the two-dimensional input space in a vector indexed over i, then the ith input I_i equals 1. Otherwise I_i equals 0; that is,

$$I_i = \begin{cases} 1 & \text{if a cue is present at the } i\text{th position,} \\ 0 & \text{otherwise.} \end{cases} \tag{2}$$

All cues input to the model are delayed by 50 ms to simulate the approximate visual response latency of PPC (Bisley et al., 2004). All neural processing latencies to cue onsets and offsets are affected by this delay.

Model inputs I_i are in allocentric coordinates, to allow for a stable representation of the input space through simulations. The earliest stages of the model, however, correspond to PPC, which represents visual space in retinotopic coordinates modulated by gain fields. In order for PPC to use the appropriate coordinate system, a mapping $W^R_{ij\varepsilon}$ is applied to the model input that transforms cue representations, based on the eye-position index $\varepsilon \in [1, \ldots, 81]$, which stores the position of the eyes at all times, into retinotopic space:

$$W^R_{ij\varepsilon} = \begin{cases} 1 & \text{if } i + [41 - \varepsilon]^+ = j + [\varepsilon - 41]^+ \\ 0 & \text{otherwise.} \end{cases} \tag{3}$$

Here, and throughout the remainder of the equations, $[x]^+$ represents half-wave rectification; the expression has the value of x when x is positive, and 0 otherwise. This transformation represents the coordinate mapping which occurs through visual transduction by the retina. This mapping, along with its inverse $W^C_{ij\varepsilon}$, which maps from retinotopic to craniotopic coordinates:

$$W^C_{ij\varepsilon} = \begin{cases} 1 & \text{if } i + [\varepsilon - 41]^+ = j + [41 - \varepsilon]^+ \\ 0 & \text{otherwise,} \end{cases} \tag{4}$$

is used at several points throughout the model. All simulations begin with gaze directed close to the center of the input space ($\varepsilon = 40$), although model performance is not dependent upon initial eye position. The value of ε is updated so that it reflects the new eye position whenever a saccade is produced. Saccades occur when any SC cell's activity C_i is greater than the threshold $\theta = 0.3$, as described in greater detail in subsequent sections.

4.3. Parietal area 7a

Inputs I_i first excite cells in the model's parietal area 7*a*, which processes inputs so that a transient onset response is produced. This transient is caused by a feedforward inhibitory interneuron (Grossberg, 1970). Accordingly, two populations of cell activities P^X_i and P^Y_i, are connected by a population of inhibitory interneuronal activities P^I_i (Fig. 18(A)). The input-receiving activities P^X_i are defined by the membrane equation:

$$\frac{1}{10}\frac{dP^X_i}{dt} = -P^X_i + (1 - P^X_i)\left[\sum_j W^R_{ij\varepsilon} I_i\right]. \tag{5}$$

In Eq. (5), a passive decay term $-P^X_i$ causes activity to decrease toward zero in the absence of input, and a shunted excitatory signal $\sum_j W^R_{ij\varepsilon} I_i$ serves as the model's input. This term represents the first coordinate remapping (discussed above) which transforms inputs I_i from their initial allocentric coordinate system to a retinotopic coordinate system through the map $W^R_{ij\varepsilon}$ (Eq. (3)).

Activities P^X_i excite inhibitory interneuronal activities P^I_i which are also described by a similar membrane equation:

$$\frac{1}{10}\frac{dP^I_i}{dt} = -P^I_i + (1 - P^I_i) f_1(P^X_i). \tag{6}$$

In Eq. (6), a passive decay balances a shunted excitatory input signal $f_1(P^X_i)$ with a faster-than-linear signal function:

$$f_1(x) = \begin{cases} x^2 & \text{for } x \geq 0.1, \\ 0 & \text{for } x < 0.1. \end{cases} \tag{7}$$

Because of the threshold 0.1 in Eq. (7), small activities P^X_i cannot excite interneuronal activities P^I_i, and because $f_1(P^X_i)$ is faster-than-linear beyond the threshold, rising values of P^X_i quickly produce strong inputs to activities P^I_i. Consequently, when a cue is presented, interneuronal activities P^I_i are initially not activated but, after a delay, become strongly active.

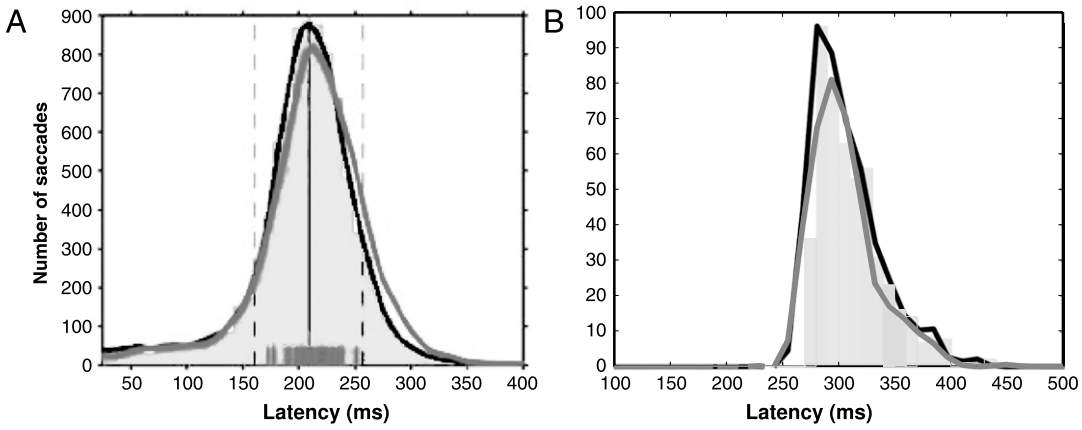

Fig. 15. Under some conditions microstimulation does not change latency. Each panel depicts histograms of control trial latencies. Curves represent kernel density function for control (black) and microstimulation (gray) latency distributions. (A) Saccade latency data demonstrating that microstimulation did not alter saccade latency. (B) Model latency data showing that latency is unchanged during simulations as well.
Source: Data adapted with permission from Histed and Miller (2006).

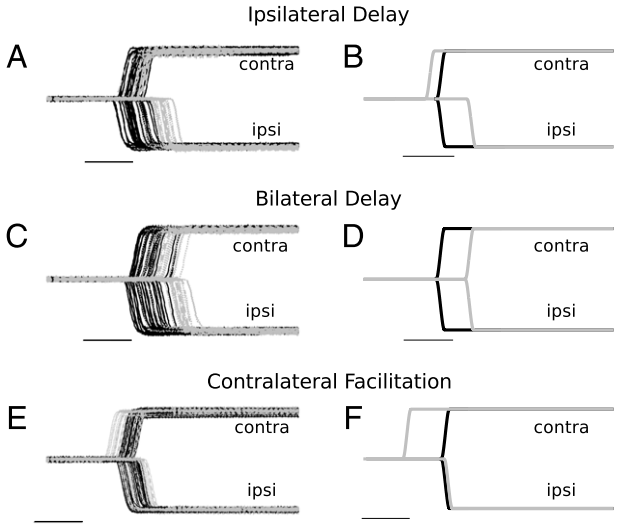

Fig. 16. SEF microstimulation can change saccade latency. Eye movement data (left) and model simulations (right) from three microstimulation sites demonstrate that, under some conditions, SEF microstimulation (gray) alters latency compared to controls (black). (A and D) A site at which late microstimulation delays ipsiversive saccades. (B and E) A site at which late microstimulation delays all saccades. (C and F) A site at which early microstimulation facilitates contraversive saccades. Saccade latency changes in these simulations, but not in Histed and Miller (2006), because of the proximity of microstimulation to saccade initiation.
Source: Data adapted with permission from Yang et al. (2008).

Both populations of cells defined above project to cells whose activities P_i^Y are described by the membrane equation:

$$\frac{1}{10}\frac{dP_i^Y}{dt} = 0.2P_i^Y + (1 - P_i^Y)20f_1(P_i^X) - 300P_i^Y(P_i^I)^2. \tag{8}$$

Weak passive decay, $-0.2P_i^Y$, allows P_i^Y to be activated quickly by a shunted excitatory input $f_1(P_i^X)$. Each transient onset cell receives a delayed *inhibitory input* $(P_i^X)^2$ that truncates the transient elevation in the activity P_i^Y, which marks the onset of visual cues. Following the onset response, 7*a* cells continue to fire in response to cue inputs, but activity P_i^Y is below the threshold required to excite WM cell activities M_{ir}, to which 7*a* cells project. The activities P_i^Y serve as the primary driving inputs to the WM. A transient onset response is important when instating an item into WM because WM representations depend not only on the spatial position of cues, but also on their rank. Without transient onset activity, when more than one cue is present simultaneously multiple representations would be instated into WM with the same rank information. The use of transient onset signals avoids this problem because even cues that overlap in time can be represented as temporally separable bursts of activity. When PPC cue representations are separated in time, each can be bound to a particular rank independently.

4.4. Lateral intraparietal cortex

The model PPC also contains lateral intraparietal (LIP) neurons with activities P_i^L. When cues are presented, cells in this population retain representations until the cues are extinguished. These cells are directly comparable to the PPC cells used in the TELOS model (Brown et al., 2004), which showed how cells in PPC and FEF cooperate and compete to open BG gates, enabling the oculomotor system to balance between reactive and planned saccades, as discussed in Section 2.5. The model LIP cell activities obey the membrane equation:

$$\frac{1}{10}\frac{dP_i^L}{dt} = -P_i^L + (1 - P_i^L)\left[4f_2(P_i^Y) + 2F_i^O + f_3(P_i^L)\right] - P_i^L\left[1 + \sum_{k\neq i}\left(100([P_k^L]^+)^4 + 0.3F_k^O\right)\right]. \tag{9}$$

These cells receive complex sets of excitatory and inhibitory inputs. The excitatory input $4f_2(P_i^Y) + 2F_i^O + f_3(P_i^L)$ consists of three terms. The first carries the driving visual information from area 7*a* cell activities P_i^Y whose signals are shaped by the sigmoid signal function:

$$f_2(x) = \frac{x^2}{0.2^2 + x^2}. \tag{10}$$

This signal function ensures that lower activity levels P_i^Y, which follow the transient onset response, are able to excite LIP cells so LIP representations reflect the continuing presence of inputs. The second excitatory term, from FEF output layer cell activities F_i^O, excites LIP cells so that FEF and PPC can reach a state of consistent coherence between planning representations that is required for the production of volitional saccades (see Brown et al., 2004). Finally, model LIP cells have a recurrent on-center term $f_3(P_i^L)$, where

$$f_3(x) = \frac{x^3}{0.4^3 + x^3}, \tag{11}$$

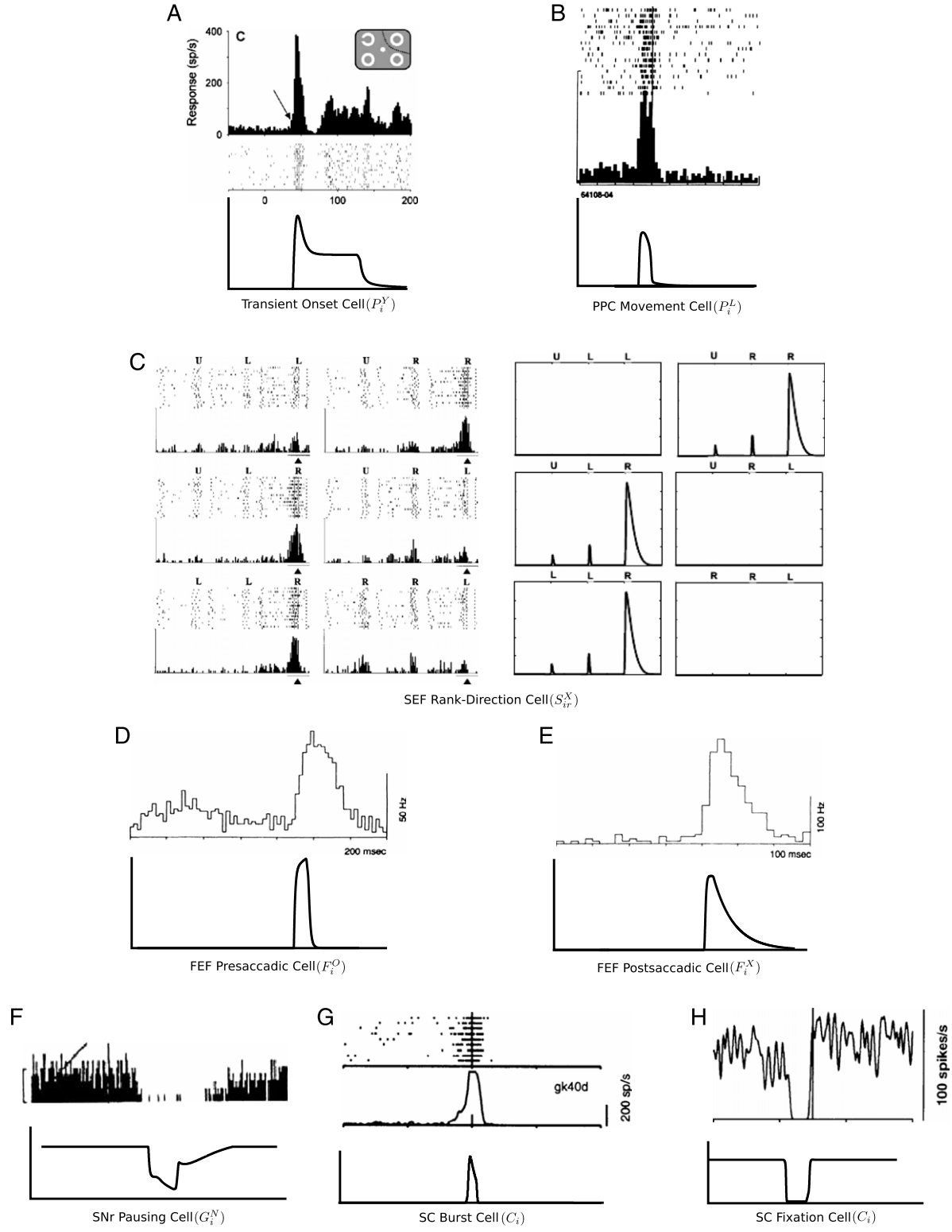

Fig. 17. Examples of electrophysiological cell types reproduced by model activity. In each case, model traces are paired with experimental data. (A) Model PPC transient onset cell activities P_i^Y respond transiently to the initial presentation of the stimulus and subsequently exhibit lower firing rates. (Data adapted with permission from Bisley et al., 2004.) (B) Movement cell activities P_i^L in PPC fire transiently prior to the initiation of a visually-guided saccade. (Data adapted with permission from Colby et al., 1996.) (C) SEF rank-direction cell activities S_{ir}^X increase phasically before saccades initiated to a preferred spatial position when the saccade occurs at a preferred ordinal position in a sequence. Model activities are compared to a cell that responds preferentially to rightward saccades that occur at the third ordinal position. (Data adapted with permission from Isoda & Tanji, 2002.) (D) FEF presaccadic cells burst before saccades of their preferred direction and amplitude. Model FEF output layer cell activities F_i^O increase phasically before saccades as well. (Data adapted with permission from Schall, 1991.) (E) Model postsaccadic cell activities F_i^X are excited by SC cells after saccades and passively decay back to baseline. (Data adapted with permission from Schall, 1991.) (F) Real SNr cells pause before saccades toward their preferred direction just as model SNr cell activities G_i^N pause to relieve SC cells from inhibition so saccades can occur. (Data adapted with permission from Hikosaka & Wurtz, 1989.) (G) Real and model SC burst cells fire phasically before saccades. (Data adapted from Munoz & Wurtz, 1995.) (H) SC fixation cells fire while fixation is maintained at a target and pause during saccades. The model SC cell C_i that corresponds to the center of the input space, in retinotopic coordinates, behaves like a fixation cell. Data adapted with permission from Munoz & Wurtz, 1993.

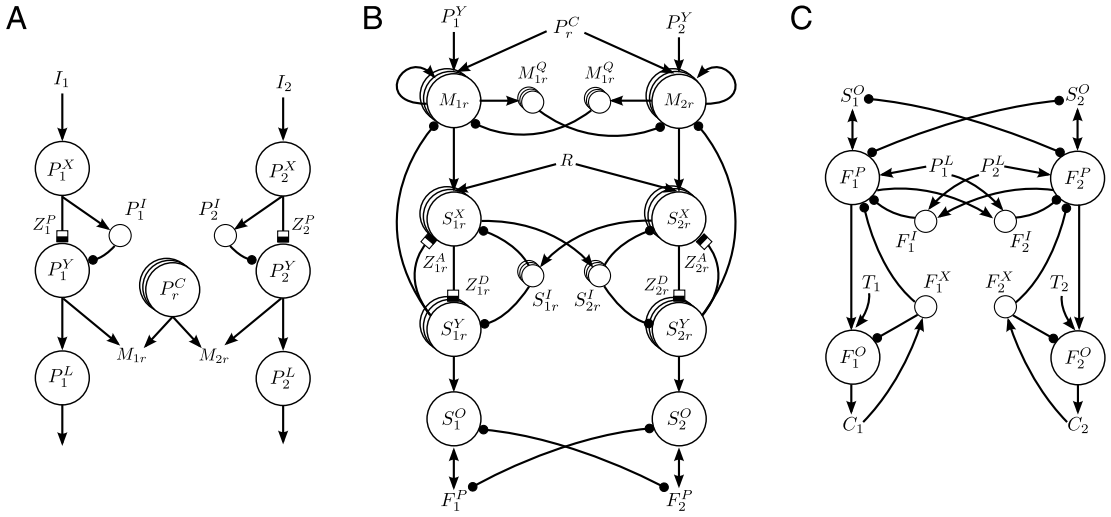

Fig. 18. Circuit diagrams for parietal and frontal cortices. For simplicity, only two competing channels are shown. (A) Circuit diagram for posterior parietal cortex, including area 7*a*, lateral intraparietal cortex and superior parietal lobule counting cells. (B) Local circuit diagram of prefrontal cortex, which contains the working memory, and the supplementary eye field, which selects plans from memory. Prefrontal cortex and the supplementary eye fields interact heavily and form an Item-Order-Rank system. (C) Circuit diagram for frontal eye fields. Plan layer cells try to excite output layer cells, but need a BG gate to open first. Output layer cells excite superior colliculus to generate saccades.

which enables them to support their own activation as they inhibit neighboring cells via a recurrent off-surround $\sum_{k\neq i} 100([P_k^L]^+)^4$. This recurrent on-center off-surround network facilitates the selection of cells consistent with a simple, coherent, plan, as is normally required for BG gate opening and saccade production.

The inhibitory signals $\sum_{k\neq i}\left(100([P_k^L]^+)^4 + 0.3F_k^O\right)$ in Eq. (9) embody a competition among saccade plans both within LIP, and between LIP and FEF. The off-surround $\sum_{k\neq i} 100([P_k^L]^+)^4$ inhibits LIP cells at different spatial positions. The second term $0.3\sum_{k\neq i} F_k^O$ enables FEF cells to inhibit cue representations in LIP as part of the competition which leads to consistent coherence between planning representations in the two regions.

Model LIP cells, because of their high degree of interconnectivity with FEF, are key participants in the gate-opening process. If a saccade is to be executed to position i, the cell activity P_i^L must increase, and other cells must reduce their activities, to ensure that the oculomotor system is prepared to execute the selected plan.

4.5. Counting cells

The PPC counting cells are found in SPL (Sawamura et al., 2002); see Fig. 1. These cells, as described in Section 2.1, fire strongly when an event occurs at a preferred ordinal position, or rank, within a sequence of events. Model counting cell activities P_r^C thus have a preferred rank r. While the first item is being instated into WM, the cell with preferred rank $r = 1$ is active ($P_1^C = 1$) while all other cells are inactive ($P_{q\neq 1}^C = 0$). When the second item is being instated into WM, only the cell activity P_2^C is excited, and so on. Each time an item is added to the spatial WM, the counting cell population is adjusted so that it reflects the rank order of the item being added in the current task trial. If a three-node SPL population is used, then the counting cell activities correspond to rank as in Table 1 (Section 2.1). The model's counting cell population is updated algorithmically during simulations, for simplicity. See Grossberg and Repin (2003) for a neural model of how parietal counting cells may be updated.

Together these three components, parietal areas 7*a*, LIP and SPL, form the model's first stage for processing visual event sequences (Fig. 18(A)). Cells in area 7*a* generate transient onset responses that are combined with counting cell activity from SPL to produce rank-augmented representations of cues within a rank-sensitive WM. Neurons in 7*a* also excite cells in LIP that remain active as long as inputs are present, and thereby participate in a cooperative–competitive interaction with FEF until the two oculomotor regions reach a state of consistency between the highly active planning representations, which coherently drive downstream oculomotor systems to generate eye movements.

4.6. Rank-sensitive craniotopic spatial working memory

The model WM is implemented by a two-layer recurrent network (e.g. Grossberg & Pearson, 2008). One layer is composed of excitatory WM cell activities M_{ir} and a second is composed of inhibitory interneuronal activities M_{ir}^Q that are responsible for the competition that creates the primacy gradient which encodes the order of the items in the sequence. Recurrent self-excitatory feedback within the excitatory layer stores this order in WM. Each of these cells is rank-sensitive. Every spatial position i possesses multiple cells, each with its own preferred rank r. Fig. 2 shows how item, order, and rank information are combined in this spatial WM. These populations represent the visual field in craniotopic coordinates, rather than retinotopic coordinates.

The activities M_{ir} obey the membrane equation:

$$\begin{aligned}\frac{dM_{ir}}{dt} &= -0.1M_{ir} + (1 - M_{ir}) \\ &\quad\times \left[2\mu W_i^P P_r^C \sum_j W_{ij\varepsilon}^C f_5(P_i^Y) + 0.7 f_4(M_{ir})\upsilon_{ir}\right] \\ &\quad - M_{ir}\left[0.4\sum_{kq\neq ir} M_{kq}^Q + 1000[S_{ir}^Y - 0.5]^+\right]. \end{aligned} \tag{12}$$

The slow passive decay rate, which facilitates WM storage, is defined by $-0.1M_{ir}$. The excitatory term $2\mu W_i^P P_r^C \sum_j W_{ij\varepsilon}^C f_5(P_i^Y)$ represents bottom-up input from PPC, which instates cue representations into WM. Term μ gates PPC inputs:

$$\mu = \begin{cases} 1 & \text{if the task utilizes working memory} \\ 0 & \text{otherwise.} \end{cases} \tag{13}$$

Through this parameter, the excitability WM cell activities M_{ir} is manipulated: when $\mu = 1$, it is possible for cues to be

instated into working memory, but when $\mu = 0$ cues cannot be instated because WM cells are rendered unexcitable. This parameter is used to remove WM from the system, representing observations that prefrontal cells that would be active during WM delay intervals are not active when task demands to not include memory requirements (Fuster, 1973; Kojima & Goldman-Rakic, 1984). As described in Section 2.2, this gate represents the learned ability of the brain to control the flow of information into WM, which has emerged as an important neural competency (Awh & Vogel, 2008, McNab & Klingberg, 2008). Further control over the flow of information into WM is represented by term W_i^P, a weight matrix with all values set to 1 except for $i = 41$ which is set to 0:

$$W_i^P = \begin{cases} 1 & \text{for } i \neq 41 \\ 0 & \text{for } i = 41. \end{cases} \tag{14}$$

These weights stop fixation-related activity from exciting WM cells, while allowing all cues that must be remembered for task success to be instated into WM. The activity P_r^C represents binary-valued inputs from SPL counting cells (Table 1). Term $\sum_j W_{ij\varepsilon}^C f_5(P_i^Y)$ thresholds the parietal onset response activities P_i^Y through the signal function:

$$f_5(x) = \begin{cases} x & \text{for } x \geq 0.4 \\ 0 & \text{for } x < 0.4 \end{cases} \tag{15}$$

and then transforms them from retinotopic to craniotopic coordinates via the mapping $W_{ij\varepsilon}^C$ (Eq. (4)). Onset responses are required because when item representations overlap in time, each would otherwise be instated into WM with the same rank. The resulting input from parietal cortex is a thresholded copy of area 7*a* activity P_i^Y that is remapped into craniotopic coordinates, augmented with rank information, and with fixation-related activity removed. If a cue is presented as the first item in a sequence ($r = 1$), and is at a spatial position $i \neq 41$ other than fixation, a transient signal excites the corresponding WM cell activity M_{i1} thereby instating a rank-sensitive representation of that cue into WM. If a second cue is presented at a spatial position $j \neq 41$, a transient signal excites the WM cell activity M_{j2} and instates a second rank-sensitive representation into WM. If these two cues are at the same spatial location ($i = j$) the two WM representations can be differentiated on the basis of their ranks, and can therefore be represented by different WM cells.

Recurrent self-excitatory feedback is defined by $0.7 f_4(M_{ir}) \upsilon_{ir}$, and is balanced by the recurrent off-surround $0.4 \sum_{kq \neq ir} M_{kq}^Q$ where the inhibitory interneurons, with activity M_{ir}^Q, track the values of excitatory WM cells:

$$\frac{dM_{ir}^Q}{dt} = -0.1 M_{ir}^Q + (1 - M_{ir}^Q) 0.2 M_{ir}. \tag{16}$$

These interneurons are also subject to passive decay and receive shunted excitatory inputs from the primary WM activities M_{ir}. The interneurons and excitatory neurons together form the WM (see Figs. 1 and 16(B)) which produces and maintains rank-selective representations of spatial cues in an activity gradient that can drive the production of a sequence of saccades to remembered target locations.

Self-excitatory feedback within WM is thresholded by the signal function

$$f_4(x) = \begin{cases} x & \text{for } x \geq 0.05 \\ 0 & \text{for } x < 0.05, \end{cases} \tag{17}$$

which ensures that, once items are deleted following selection, small values of M_{ir} do not lead to the false reappearance of WM traces. The strength of the positive feedback is scaled by the value υ_{ir}, which represents normally distributed pseudorandom noise with mean 1 and standard deviation 1. As a result, auto-excitatory feedback at each time step varies slightly, introducing noise into the WM traces. Because of noise, similar activity levels of two WM item representations can lead to selection of items in the wrong order. This stochasticity is required to reproduce the results described by Histed and Miller (2006), because several simulations are used to estimate the effect of microstimulation in probabilities, as well as many other data about WM storage (Grossberg & Pearson, 2008). After a stored item is selected, the strong inhibitory signal $1000[S_{ir}^Y - 0.5]^+$ from SEF cell activities S_{ir}^Y deletes that item representation from WM.

4.7. Supplementary eye field cell populations

The model SEF consists of four populations of cells that form a habituative recurrent on-center off-surround network which selects saccade plans from WM and excites corresponding representations in FEF for execution, when task conditions permit (Fig. 18(B)). Two populations of rank-sensitive excitatory cells, with membrane activities S_{ir}^X and S_{ir}^Y, form the habituative recurrent on-center. They are reciprocally connected through descending and ascending habituative gates Z_{ir}^D and Z_{ir}^A, respectively. A third population of rank-sensitive inhibitory interneuronal activities S_{ir}^I forms the recurrent off-surround that drives a winner-take-all competition among item representations in WM. The output population consists of rank-insensitive activities S_i^O that receive inputs from item *i*, irrespective of rank, and excite corresponding plans in FEF.

Onset of the rehearsal period is indicated by the disappearance of the fixation point and signaled by the consequent excitation of the model's ventral anterior thalamic nucleus *R* (Fig. 10(D)) (Huerta & Kaas, 1990; Shook, Schlag-Rey, & Schlag, 1991) through opening of a BG gate (Fig. 4(A); see Section 4.13). The SEF then selects the most active representation in WM. In particular, SEF activities S_{ir}^X are described in the equation:

$$\frac{dS_{ir}^X}{dt} = -2S_{ir}^X + (1 - S_{ir}^X)\left[\varsigma_i + 0.9 f_4(M_{ir}) R + 10 Z_{ir}^A (S_{ir}^Y)^2\right] - S_{ir}^X f_2(S_{ir}^I). \tag{18}$$

In Eq. (18), a fast passive decay term $-2S_{ir}^X$ enables SEF cells to equilibrate quickly when a saccade plan is selected and excited in FEF, in order to stage another competition and select the next saccade plan. The excitatory inputs in Eq. (18) are broken into three terms. The first term ς_i represents microstimulation. On tasks in which microstimulation is applied to SEF (e.g. Histed & Miller, 2006; Yang et al., 2008), this term excites cells with a two-dimensional Gaussian kernel that is described in greater detail in Section 4.8. The second term $0.9 f_4(M_{ir}) R$ represents the driving input from WM cell activities M_{ir}, thresholded by the signal function $f_4(x)$ in Eq. (17), and modulated by the BG gate *R*; see Eq. (38). The third excitatory term $10 Z_{ir}^A (S_{ir}^Y)^2$ represents feedback from rank-sensitive SEF cells S_{ir}^Y modulated by habituative gates Z_{ir}^A which obey:

$$\frac{dZ_{ir}^A}{dt} = 0.01(1 - Z_{ir}^A) - Z_{ir}^A\left[(S_{ir}^Y)^2 + 25(S_{ir}^Y)^4\right]; \tag{19}$$

cf. Gaudiano and Grossberg (1991). The gate is habituated by two terms: one that corresponds to the signal $(S_{ir}^Y)^2$ that passes through the gate, and a second $25(S_{ir}^Y)^4$ that corresponds to the square of the signal, so that habituation accelerates at higher activation levels. The SEF input cell activities S_{ir}^X in Eq. (18) also receive an inhibitory input $f_2(S_{ir}^I)$ from SEF interneuronal activities S_{ir}^I shaped

by the sigmoid signal function $f_2(x)$ described by Eq. (10). These SEF interneurons are excited by SEF input layer activities S^X_{ir}:

$$\frac{1}{10}\frac{dS^I_{ir}}{dt} = -2S^I_{ir} + (1 - S^I_{ir})\left[\varsigma_i + 2\sum_{kq\neq ir} f_7(S^X_{kq})\right]. \quad (20)$$

Like the SEF input layer cells, SEF interneurons have fast passive decay rates that enable fast reset after selection. Their excitatory inputs comprise microstimulation ς_i, modeled by the same two-dimensional Gaussian kernel, and the excitatory input $2\sum_{kq\neq ir} f_7(S^X_{kq})$ from SEF input layer cells, as shaped by the sigmoid signal function:

$$f_7(x) = \frac{x^4}{0.5^4 + x^4}. \quad (21)$$

These inhibitory interneurons form a broad off-surround by receiving excitatory input from all other spatial positions $kq \neq ir$. Thus, interneurons are excited whenever there is activity in the input layer at spatial positions other than their own. This allows the most active input field cell to silence all others and win the competition.

These two cell types also participate in a feedforward competition, which facilitates the process of habituation, because cells in multiple layers must interact to select the strongest WM representation. In addition, the dynamics of feedforward completion allows the strengths of *all* representations to increase at the beginning of the competition. That all cells, including those that ultimately lose the competition, increase their activity at the beginning of each selection provides a more accurate match to SEF electrophysiological data, which sometimes shows cells that fire weakly prior to saccades to nonpreferred spatial locations (Isoda & Tanji, 2002, 2003; Lu et al., 2002). Feedforward competition occurs via off-surround inhibition of excitatory cell activities S^Y_{ir} with membrane equations

$$\frac{1}{10}\frac{dS^Y_{ir}}{dt} = -2S^Y_{ir} + (1 - S^Y_{ir})\left[\varsigma_i + 25Z^D_{ir}(S^X_{ir})^2\right] - 15S^Y_{ir}f_2(S^I_{ir}); \quad (22)$$

see Fig. 18(B). This population of excitatory cells has activity similar to input cell activities S^X_{ir}. Its cells have a high rate of passive decay and are excited by microstimulation through the term ς_i. The second excitatory term $25Z^D_{ir}(S^X_{ir})^2$ represents the primary excitatory input: a one-to-one habituating signal, through feedforward habituative gates Z^D_{ir}, from input cell activities S^X_{ir}. The habituative gates obey:

$$\frac{dZ^D_{ir}}{dt} = 0.1(1 - Z^D_{ir}) - Z^D_{ir}\left[(S^X_{ir})^2 + 20(S^X_{ir})^4\right]. \quad (23)$$

Through these gates, which also depend on the signal $(S^X_{ir})^2$ and its square, $20(S^X_{ir})^4$, and the feedback habituative gates Z^A_{ir} in Eq. (19), the two populations of rank-sensitive excitatory SEF cell activities S^X_{ir} and S^Y_{ir} are reciprocally connected by mutually excitatory one-to-one connections. The feedforward competition between these two fields is due to this one-to-one excitation combined with off-surround inhibition from the interneuronal activities S^I_{ir} (Eq. (20)), represented by the inhibitory term $-15S^Y_{ir}f_2(S^I_{ir})$.

These three rank-selective fields form a winner-take-all circuit (Fig. 18(B)) which utilizes both recurrent and feedforward competition to select the most active representation from their WM cell inputs M_{ir}. WM representations, once the gate R opens, excite their corresponding SEF selection cell activities S^X_{ir}, which in turn excite cell activities S^Y_{ir} in the second selection layer. These cells then reinforce one another's activity through reciprocal excitatory connections, and inhibit other selection cells through the interneuronal activities S^I_{ir}, thereby reducing the strength of competing representations. Ultimately, the strongest representation is chosen and all other representations become strongly inhibited. Once one representation wins, the uninhibited reciprocal connections between the excitatory selection cells cause the strength of the winning representation to further increase. As the strength of this representation increases, selection cell activities S^Y_{ir}, through the inhibitory feedback in Eq. (12), delete the selected representation from WM. This inhibition-of-return mechanism is rank-sensitive and prevents perseveration on a single choice without interfering with the system's ability to perform the same item at a later rank. In addition, the winning selection cells continue to excite each other until the habituative gates, Z^D_{ir} and Z^A_{ir}, that control their mutual excitation, are depleted to such an extent that their continued activation can no longer be sustained. At this point, SEF selection activity subsides autonomously, and the system becomes able to make a new selection. This autonomous shut-off, made possible by the habituation, is important because later stages are rank-insensitive, hence incapable of sending a rank-sensitive shut-off signal to SEF. In summary, there are three types of rank-sensitive SEF cells. In this version of the model, their rank-sensitive activity depends on rank-sensitive inputs from PFC. The model has no direct inputs from SPL counting cells to SEF.

A fourth population of SEF cell activities S^O_i is rank-*insensitive*, and responsible for exciting the selected saccade plan, without regard to rank, in FEF and ultimately the remaining components of the oculomotor hierarchy (Fig. 18(B)). These cells obey the membrane equation:

$$\begin{aligned}\frac{1}{10}\frac{dS^O_i}{dt} = {} & -S^O_i + (1 - S^O_i)\left[\left(\varsigma_i + 10\sum_r f_8(S^Y_{ir})\right)\right. \\ & \left.\times\left(1 + 1.5\sum_j W^C_{ij\varepsilon} f_3(F^P_i)\right)\right] \\ & - 0.6S^O_i\left[\sum_{k\neq i}\sum_j W^C_{kj\varepsilon} f_3(F^P_i)\right]. \end{aligned} \quad (24)$$

As with all other SEF cells, microstimulation is a source of shunted excitation through the term ς_i. The driving excitatory input to these output cells, $10\sum_r f_8(S^Y_{ir})$, is a sum of signals from all selection cell activities S^Y_{ir} that share the same preferred rank r. These excitatory signals are passed through the Heaviside signal function:

$$f_8(x) = \begin{cases} 1 & \text{for } x \geq 0.5 \\ 0 & \text{for } x < 0.5, \end{cases} \quad (25)$$

which thresholds and binarizes inputs from the selection system so that only winning representations, whose activities S^Y_{ir} have surpassed 0.5, impact activities S^O_i. The combined excitatory effect of microstimulation and driving inputs from activities S^Y_{ir} are modulated by feedback from FEF cell activities F^P_i (Fig. 18(B)) through the term $1+1.5\sum_j W^C_{ij\varepsilon} f_3(F^P_i)$ which, in the absence of FEF activity, has the value of 1. In the presence of FEF activity, the value of this term is increased by a factor proportional to activities F^P_i after they are shaped by the sigmoid signal function $f_3(x)$, defined in Eq. (11), to minimize the transfer of noise.

In Eq. (24), the map $W^C_{ij\varepsilon}$ (Eq. (4)) is responsible for transforming activity from the retinotopic coordinate frame, used in FEF, to the craniotopic frame used in SEF. This one-to-one excitatory feedback from FEF to the SEF output stage is responsible for facilitating the rapid transfer of information between the two regions, and acts in conjunction with an inhibitory off-surround feedback signal, implemented through the term $\sum_j W^C_{ij\varepsilon} f_3(F^P_i)$, which ensures that any activity F^P_i inconsistent with the selected representation does not excite spurious representations in SEF output cells.

In summary, the model SEF selects the most active WM activity M_{ir} through recurrent and feedforward competition, deletes the representation from WM, preserves item but not rank at its output stage, and excites a corresponding representation in FEF plan layer cell activities F_i^P. Once in FEF, as discussed below, cell activities F_i^P interact in a cooperative–competitive dynamic with LIP cell activities P_i^L, both of which place bids to the BG in an effort to open a gate to allow plan-specific signals to flow through further downstream oculomotor areas and ultimately to SC.

4.8. Supplementary eye field microstimulation

Microstimulation is modeled through a two-dimensional Gaussian kernel

$$\varsigma_i = 0.4 \exp\left[-\left(\frac{(g_x(i) - g_x(i_0))^2}{2\sigma^2} + \frac{(g_y(i) - g_y(i_0))^2}{2\sigma^2}\right)\right] \quad (26)$$

with standard deviation $\sigma = 3$. When microstimulation is applied at position i_0 microstimulation strength decreases as a Gaussian function of distance from i_0. In order to compute the Gaussian the functions $g_x(i) = \text{floor}((i-1)/9)+1$ and $g_y(i) = \text{mod}(i-1, 9)+1$ transform the subscript i into Cartesian coordinates (x, y), where the function floor (a) yields the largest integer value not greater than a and the function $\text{mod}(a, b)$ returns the remainder of the division operation a/b. The moment microstimulation is applied, the Gaussian kernel impacts all positions according to Eq. (26). The moment microstimulation ceases, all values of ς_i immediately return to zero.

The impact of microstimulation, however, can last longer than the microstimulation interval. When microstimulation excites cells, it can produce lasting effects via feedback signaling. It can also cause significant closure of the habituative gates Z_{ir}^D and Z_{ir}^A, and thereby alter how selection functions. When microstimulation is applied during the Histed and Miller (2006) task, it lasts for an interval of 900 ms, which the model proposes has the effect of habituating the SEF selection system. Habituation is strongest at the center of microstimulation and decreases as a Gaussian function of distance.

4.9. Frontal eye fields

The model FEF is excited by SEF once a saccade plan is selected from WM. The FEF comprises four retinotopic fields (Fig. 18(C)): an FEF plan layer with cell activities F_i^P, an output layer with cell activities F_i^O, a field of interneuronal activities F_i^I, and a population of postsaccadic cell activities F_i^X. The membrane equations and relationship between the plan and output layers are based upon the TELOS model (Brown et al., 2004). A saccade command enters the plan layer and tries to activate cells in the output layer but cannot until a BG gate opens. Once the gate opens, the plan can flow to the output layer, and ultimately to the SC.

Plan layer cell activities F_i^P receive their driving input from SEF output cell activities S_i^O and interact through an on-center off-surround network. They obey the membrane equation:

$$\frac{1}{10}\frac{dF_i^P}{dt} = -2F_i^P + (1 - F_i^P)\left[P_i^L + 20\sum_j W_{ij\varepsilon}^R [S_i^O - 0.2]^+\right] - F_i^P\left[2F_i^I + 5F_i^X + \sum_{k\neq i}\sum_j W_{ij\varepsilon}^R [S_i^O - 0.2]^+\right]. \quad (27)$$

Because FEF cells are characterized by short transient bursts of activity, plan cells have a high rate of passive decay $-2F_i^P$ that causes them to quickly become silent in the absence of inputs. They are the target of two excitatory projections: one from LIP cell activities P_i^L and another from SEF output cell activities S_i^O (Fig. 18(B) and (C)) which is transformed from craniotopic to retinotopic coordinates by the kernel $W_{ij\varepsilon}^R$ (Eq. (3)).

FEF plan cells are inhibited by three separate sources. First, they are inhibited by FEF interneuronal activities F_i^I that obey the membrane equation:

$$\frac{1}{10}\frac{dF_i^I}{dt} = -0.1F_i^I + (1 - F_i^I)\left[\sum_{k\neq i}\left(f_2(F_k^P) + 0.8P_k^L\right)\right]. \quad (28)$$

In Eq. (28), an off-surround projection from plan layer cell activities, $f_2(F_k^P)$ with positions $k \neq i$, in conjunction with the off-surround inhibitory projection, $0.8P_k^L$, provides a basis for a FEF recurrent competition to ensure that the plan layer holds only a single plan at a time. The projection from LIP cell activities P_k^L (again with $k \neq i$), participates in the competition between FEF and LIP, which helps the two areas to reach a consensus and open a BG gate. The second source of inhibition in Eq. (27) is a population of FEF post-saccadic cell activities F_i^X that are governed by the equation

$$\frac{dF_i^X}{dt} = -2F_i^X + (1 - F_i^X)100f_9(C_i), \quad (29)$$

where $f_9(x)$ is the Heaviside signal function

$$f_9(x) = \begin{cases} 1 & \text{for } x > \theta \\ 0 & \text{for } x \leq \theta \end{cases} \quad (30)$$

that thresholds the excitatory signal from SC cell activities C_i, according to the saccade threshold $\theta = 0.3$, and uniformizes SC activity to generate uniform post-saccadic responses. These cells fire upon the onset of suprathreshold colliculus activity and are responsible for silencing FEF saccade-related activity once the eye movement has been initiated (in a more complete model, the SC-to-FEF feedback would have a relay in the thalamus). Finally, plan layer cell activities F_i^P receive a third source of inhibition in Eq. (27): a thresholded inhibitory off-surround projection from SEF output cell activities S_i^O. Together with on-center excitatory projections between SEF and FEF, this inhibitory signal helps to ensure sharply focused transmission of saccade target information. Even in this non-distributed version of the model, its usefulness was seen in cases where SEF microstimulation excited many cells, but did not induce unfocused excitation of many plans in FEF.

Once a plan has been excited in FEF, plan layer cell activities F_i^P try to excite the deeper output layer cell activities F_i^O, though until FEF and LIP contain consistent saccade plans and open a BG gate, output layer cells remain unexcitable (as in the TELOS model; Brown et al., 2004). Output layer cells are described by

$$\frac{1}{10}\frac{dF_i^O}{dt} = -F_i^O + (1 - F_i^O)3F_i^P T_i^- 6F_i^O F_i^X. \quad (31)$$

Output layer cell activities F_i^O receive one excitatory input from plan layer cell activities F_i^P which is multiplied, or gated, by cell activities T_i in a pallidal or nigral receiving nucleus of the thalamus (Brown et al., 2004) that are disinhibited by BG gate opening. Thus, until thalamic activity T_i is non-zero, output cells remain quiescent. Output layer cells are inhibited by FEF postsaccadic cells, described in Eq. (29), so that once a saccade plan in the output layer produces suprathreshold activity in SC, FEF representations are removed to allow the next saccade plan to pass through the system.

In summary, model FEF (Fig. 18(C)) receives saccade plans from SEF that have been selected from WM. Between SEF and FEF, the plans are mapped into retinotopic coordinates so that they can be utilized by downstream areas in the oculomotor hierarchy. When plans are first excited in FEF, they reside in FEF plan layer cell activities F_i^P and prime FEF output layer cell activities F_i^O which cannot be excited until thalamic cell activities T_i are disinhibited by BG gate opening. Once output cell activities F_i^O are activated, they try to excite SC cell activities C_i but cannot until a second BG gate, described in the forthcoming pages, is opened.

4.10. Superior colliculus

Model SC consists of a population of cell activities C_i that are excited by LIP and FEF outputs which are sufficiently consistent to generate saccades. Colliculus cells follow the membrane equation:

$$\frac{dC_i}{dt} = (1 - C_i)\left[50f_7(P_i^L) + 40f_7(F_i^O)\right] - C_i\left[800[G_i^N - 0.3]^+ + 10\right]. \quad (32)$$

SC cell activities are driven in Eq. (32) by two excitatory inputs, one from LIP cell activities P_i^L, and another from FEF output cell activities F_i^O, which are passed through the signal function $f_7(x)$, described in Eq. (21), so low levels of activity in these regions do not excite SC. It is difficult to activate superior colliculus cells with these inputs unless substantia nigra cell activities G_i^N in the collicular BG loop are strongly inhibited. This is because, under baseline conditions, the substantia nigra strongly inhibits SC cells through the term $800[G_i^N - 0.3]^+$ and only releases SC cells once it is itself inhibited.

4.11. Saccade production and remapping

When SC activity C_i passes the model saccade threshold $\theta = 0.3$, a saccade is triggered. At every simulation timestep, model SC cells are checked for suprathreshold activity. If any SC cell activity C_i passes the threshold, due to excitation from FEF and LIP in the presence of reduced inhibition by BG, the system must update its representation of eye position ε to reflect the execution of a saccade. The saccade target location i, or the subscript of the SC cell activity C_i that has passed threshold, represents the new eye position in retinotopic coordinates. The spatial location i is then algorithmically mapped into craniotopic coordinates, and then assigned as the new value of ε. Once ε has been updated, the effect propagates throughout the entire model because the mappings $W_{ij\varepsilon}^R$ and $W_{ij\varepsilon}^C$ depend on ε. Any cues that are present in the environment begin exciting new cells in the model parietal areas.

4.12. Basal ganglia and gating

The model contains three separate basal ganglia (BG) loops, each of which serves as a gate to control the timing of a different function in the model. The BG are implemented as in the TELOS model (Brown et al., 2004) and each loop includes four populations of cells that represent the striatal direct and indirect pathways, the globus pallidus external segment (GPe), and the substantia nigra pars reticulata (SNr). Each loop through the BG (Fig. 4) is responsible for opening and closing a gate which is ordinarily held closed by strong inhibition emerging from SNr. Cells in the striatal direct pathway inhibit SNr cells, thereby disinhibiting thalamus or SC cells and opening the gate. Indirect pathway cells inhibit GPe cells which, in turn, inhibit SNr cells. The net effect of striatal indirect pathway excitation is a strengthening of SNr cell activation and therefore enhanced gate closure.

4.13. Gating readout from working memory

As described in Section 4.6 and Figs. 1, 18(B) and 10(D), a thalamic gate R controls output from WM. Recall that Eq. (18) describes changes in SEF input layer cell activities S_{ir}^X. The driving input to these cells comes from the WM cell activities M_{ir} but is gated by the activity of R through term $0.9f_4(M_{ir})R$. The activity of R is controlled by a loop through the BG whose indirect pathway receives input from LIP cell activities P_i^L and whose direct pathway has a constant value that pushes the gate open in the absence of indirect pathway activity. The WM loop striatal medium spiny projection neurons (MSPNs) of the direct pathway, with activities M^D, attempt to open the gate and are governed by the membrane equation:

$$\frac{dM^D}{dt} = (1 - M^D)50 - (M^D + 0.58); \quad (33)$$

see Fig. 4(A). The first term, $(1 - M^D)50$, provides a constant excitatory drive. The inhibitory term provides a static source of inhibition which controls the activity level M^D at which MSPNs equilibrate. The inhibitory term also provides the option for future modification should an inhibitory component be necessary, as is the case in other BG loops.

The direct pathway MSPNs act in opposition to the indirect pathway MSPN activities M^I which work to close the gate (Fig. 4(A)). They are characterized by the membrane equation:

$$\frac{dM^I}{dt} = (1 - M^I)\left[5\sum_i W_i^F[P_i^L - 0.25]^+\right] - (M^I + 0.58), \quad (34)$$

whereby LIP cell activities P_i^L exert their influence. The kernel W_i^F filters out activity in all LIP cell activities P_i^L, $i \neq 41$, that are not at the center ($i = 41$) of the visual field, but selectively allows activity at the center, where any object of fixation is located, to pass:

$$W_i^F = \begin{cases} 0 & \text{for } i \neq 41 \\ 1 & \text{for } i = 41. \end{cases} \quad (35)$$

The effect of this map is to produce excitation only when the system is actively fixating a cue. Because direct and indirect pathway MSPN activities M^D and M^I work in opposition to one another, the presence of a cue at the center of the visual field activates indirect pathway cells and holds the BG gate closed, whereas the absence of such a cue allows the direct pathway to push open the gate.

In order for the direct and indirect pathway MSPNs to exert their opposing goals, their activities must be integrated—a process that occurs in the two populations of GPe and SNr: GPe cell activities M^G are part of the indirect pathway, receiving a signal from indirect pathway MSPN activities M^I and obeying the membrane equation:

$$\frac{dM^G}{dt} = (1 - M^G)0.5 - (M^G + 1)\left[0.2 + 0.8[M^I]^+\right]. \quad (36)$$

The main input to these cells is a rectified inhibitory projection from the indirect pathway MSPN activities M^I. Thus, activation of indirect pathway MSPNs silences GPe activities M^G. The sole target of the GPe is the SNr activity M^N, which obeys the membrane equation:

$$\frac{dM^N}{dt} = (1 - M^N)100 - (M^N + 1)\left[54[M^D]^+ + 80[M^G]^+\right]. \quad (37)$$

In the absence of any perturbation of cell activities in the motor loop, SNr cell activities M^N are highly active because of a constant source of shunted excitation represented by the term $(1 - M^N)100$. When the direct pathway MSPN activities M^D or the GPe population activities M^G are activated, SNr cells are inhibited. The result of SNr inhibition is the disinhibition of the gate R:

$$\frac{1}{20}\frac{dR}{dt} = -0.1R + (1 - R)20[0.3 - M^N]^+, \quad (38)$$

which is strongly inhibited by SNr cell activities M^N greater than the threshold 0.3, but rapidly activates in the absence of this inhibition. In summary, this loop (Fig. 4(A)) controls the flow of information between WM cells in PFC and SEF selection cells. The direct pathway attempts to open the gate to allow selection at all times, but the presence of a cue at the center of the visual field,

indicating the task requirement of fixation, engages the indirect pathway which holds the gate closed. Once the fixation point is removed, the constant excitation of direct pathway cells forces the gate open, which allows plans to flow from WM cell activities M_{ir} to SEF input cell activities S^X_{ir}.

4.14. The FEF loop: movement of saccade plans from plan layer to output layer

Once saccade plans have been selected by the model SEF, corresponding representations are excited in FEF plan layer cell activities F^P_i (Fig. 3(A)). Plan layer cells then try to excite FEF output layer cell activities F^O_i so that the plan can excite downstream oculomotor areas and be executed (Fig. 3(C)). To ensure that only one plan is chosen for execution by the oculomotor system, a BG loop controls the flow of information between the FEF plan and output layers through the thalamic gate T_i (Figs. 4(B) and 3(C)). Recall that in Eq. (31), the gate opens only when the FEF plan layer and LIP have reached a state of coherence (Brown et al., 2004) in the sense that these two areas' most active spatial representations are not discrepant. This BG loop also contains two populations of striatal MSPNs: cell activities B^D_i that make up the direct pathway and cell activities B^I_i that make up the indirect pathway (Fig. 4(B)). Direct pathway cells use the membrane equation:

$$\frac{dB^D_i}{dt} = (1 - B^D_i)\left[3P^L_i + 20F^P_i\right] - (B^D_i + 0.58)\left[1 + 9\sum_i F^P_i\right]. \tag{39}$$

Direct pathway MSPNs in this loop are the targets of two sources of excitation: LIP cell activities P^L_i and FEF plan layer cell activities F^P_i, and a single source of inhibition: the sum of all activity $\sum_i F^P_i$ in the FEF plan layer. Because FEF and LIP are reciprocally connected through on-center off-surround pathways, analogous loci in the two areas cooperate whereas discrepant loci compete. Direct pathway MSPNs are tuned so that, once the saccade plans contained in FEF and LIP are consistent, their inputs constructively interfere and provide strong excitation. If these areas do not contain consistent saccade plans, direct pathway MSPNs are not strongly excited. Thus, the direct pathway pushes the BG gate open, to ultimately allow excitation of the FEF output layer, only when both FEF plan layer cells F^P_i and LIP cells P^L_i share the same saccade plan.

The FEF loop indirect pathway MSPN activities B^I_i act in opposition to the direct pathway MSPNs and try to keep the gate closed. Their membrane potentials are controlled by:

$$\frac{dB^I_i}{dt} = -B^I_i + 1.0, \tag{40}$$

which causes this indirect pathway to act as a constant. The indirect pathway cell activities B^I_i are at equilibrium throughout all simulations, although it is feasible that other versions of the model could use these cells to command more fine-tuned control over the passage of plans from the FEF plan layer to the FEF output layer. Indeed, TELOS and other BG loops in this model utilize this capability. Just as indirect pathway MSPN activities B^I_i serve as constants, the GPe cell activities B^G_i that make up the second stage of the indirect pathway also serve as constants, since the constant-valued indirect pathway cell activities B^I_i serve as their sole source of input (Fig. 4(B)). Their membrane activities are described by:

$$\frac{dB^G_i}{dt} = (1 - B^G_i)0.5 - (B^G_i + 1)\left[0.12 + 0.08[B^I_i]^+\right], \tag{41}$$

where $[B^I_i]^+$ is a rectified signal from striatal indirect MSPN cells that inhibits GPe cell activities B^G_i, with the net effect of disinhibiting the output SNr cell activities B^N_i.

The SNr cell activities B^N_i combine activity from striatal direct MSPN activities B^D_i and from indirect pathway GPe cell activities B^G_i and are ultimately responsible for controlling the opening of the FEF loop's thalamic gate T_i (Fig. 4(B)). The SNr cell activities B^N_i obey the membrane equation

$$\frac{dB^N_i}{dt} = (1 - B^N_i)100 - (B^N_i + 1)\left[54[B^D_i]^+ + 80[B^G_i]^+\right]. \tag{42}$$

In the absence of signals from the direct and indirect pathways, SNr cell activities B^N_i are tonically active due the constant excitatory term $(1 - B^N_i)100$. Direct pathway MSPN activities B^D_i provide a rectified inhibitory signal that causes SNr cells to pause, releasing the thalamic gate activities T_i from inhibition. The indirect pathway provides a source of inhibition, through the second inhibitory term, which consists of a rectified input from activities B^G_i. In this loop, since the activity of the indirect pathway is constant throughout all simulations, the term $80[B^G_i]^+$ simply serves as a constant. At equilibrium, the activation of SNr cell activities B^N_i remains at a balance between constant excitatory and inhibitory sources. Once FEF and LIP dynamics evolve to favor spatially compatible plans, they activate direct pathway MSPN activities B^D_i beyond an emergent threshold which disrupts the balance between inhibition and excitation in SNr cell activities B^N_i and causes a dramatic reduction in activation level.

Once the FEF loop SNr cell activities B^N_i have been inhibited through direct pathway activation, thalamic cell activities T_i, described by the membrane equation

$$\frac{1}{15}\frac{dT_i}{dt} = -0.1T_i + (1 - T_i)10[0.3 - B^N_i]^+, \tag{43}$$

are relieved from their ordinary state of inhibition and allow FEF plan layer cell activities F^P_i to excite FEF output layer cell activities F^O_i (Fig. 3(B)). The fast integration rate in Eq. (43), ensures that the opening of this gate occurs rapidly as soon as SNr cell activities B^N_i exceed the threshold 0.3.

By controlling the flow of plan signals between the FEF plan and output layers, this loop ensures that the model can balance between planned and reactive saccades (see TELOS; Brown et al., 2004). Without such a mechanism, the oculomotor system could send inconsistent plans to downstream areas, which could lead to saccadic averaging or other undesirable consequences.

4.15. Collicular loop: gating excitation of superior colliculus and saccade production

Once saccade signals have successfully passed from the FEF plan layer to the FEF output layer, FEF output cell activities F^O_i operate in tandem with LIP cell activities P^L_i to excite SC cell activities C_i and generate a saccade. This process is controlled by a third BG loop, the collicular loop (Fig. 4(C)), as can be seen by the presence of strong inhibition from SNr cell activities G^N_i in colliculus cell activities C_i, described by Eq. (32). Like the other BG loops, the collicular loop contains two populations of MSPNs that form the direct and indirect pathways responsible for opening and closing the gate, respectively. The collicular direct pathway MSPN activities G^D_i are described by the membrane equation:

$$\frac{dG^D_i}{dt} = (1 - G^D_i)\left[50[P^L_i - 0.25]^+ + 100f_{10}(F^O_i)\right] - (G^D_i + 0.58)\left[1 + 20\sum_j [P^L_j - 0.25]^+ + f_{10}(F^O_i)\right], \tag{44}$$

which combines a number of excitatory and inhibitory inputs to provide a secondary stage of assurance that the plans in the FEF

output layer and LIP are coherent. The excitatory input consists of two terms, one that represents a thresholded and rectified input from LIP cell activities P_i^L and a second that represents FEF output cell activity F_i^O, passed through the sigmoid signal function

$$f_{10}(x) = \frac{x^{10}}{0.4^{10} + x^{10}}, \tag{45}$$

which forces FEF output cell activities F_i^O to become significantly activated before they can activate MSPNs. The inhibitory inputs consist of the sum of activity across all LIP cell activities P_j^L (after being thresholded and rectified) and the sum of activity across all FEF output field cell activities F_j^O, again passed through the steep sigmoid signal function $f_{10}(x)$.

The MSPN activities G_i^I in the collicular loop indirect pathway are implemented in the same way as those of the WM loop described above. Activated only by a centrally located cue in the visual field, they hold the gate closed during fixation. Indirect pathway MSPN activity levels G_i^I change according to the membrane equation:

$$\frac{dG_i^I}{dt} = (1 - G_i^I)\left[5W_i^F[P_i^L - 0.25]^+\right] - (G_i^I + 0.58), \tag{46}$$

where W_i^F represents the map, described in Eq. (35), that filters out all activity in cells at locations $i \neq 41$, while allowing that which occurs in the cell at location $i = 41$, representing the center of the visual field. This map is applied to the thresholded and rectified LIP cell activities P_i^L so that indirect pathway MSPN activities G_i^I are excited, strengthening gate closure, only by activity corresponding to a central cue on which fixation should be maintained. These indirect pathway MSPNs are also subject to a constant source of inhibition which ensures that, in the absence of a fixation cue, activity quickly dies off, allowing direct pathway MSPN activities G_i^I to open the gate.

Indirect pathway MSPNs project to the second stage of the indirect pathway, GPe cell activities G_i^G (Fig. 4(C)) which are similar to those described in the other BG loops:

$$\frac{dG_i^G}{dt} = (1 - G_i^G)0.5 - (G_i^G + 1)\left[0.2 + 0.8[G_i^I]^+\right]. \tag{47}$$

Normally active, due to the balance between excitation and inhibition, these cells are inhibited by a rectified input from indirect pathway MSPN activities G_i^I. When inhibited in response to increased activity G_i^I, these cells release SNr output neuron activities G_i^N, from inhibition. As a consequence, the activity of SNr cells increases and the gate is forced closed.

The loop output cell activities G_i^N, which represent the SNr, are also implemented in the same way they are in other BG loops, by the membrane equation:

$$\frac{dG_i^N}{dt} = (1 - G_i^N)100 - (G_i^N + 1)\left[54[G_i^D]^+ + 80[G_i^G]^+\right], \tag{48}$$

where term $(1 - G_i^N)100$ represents a strong constant source of excitation that opposes two sources of inhibition. The first is a rectified signal from direct pathway MSPN activities G_i^D, and the second is a rectified signal from the indirect pathway GPe cell activities G_i^G which, under baseline conditions, provides a source of inhibition which can be removed by indirect pathway MSPN activation to strengthen gate closure. SC cell activities C_i, already described in Section 4.10, and by Eq. (32), cannot be activated until SNr cell activities G_i^N are sufficiently inhibited.

The collicular BG loop, like the FEF loop, detects consistency between FEF and LIP and opens a gate in response, although with the added constraint that the system is not already actively maintaining fixation at a central cue. By using two BG loops, first to control the flow of saccade plan signals from the FEF plan layer to the FEF output layer, and second to control the flow of plan signals to saccade-generating areas such as SC, the system is capable of preparing a response in advance of the disappearance of the fixation point. Once the fixation point is removed, the activation of the collicular loop indirect pathway is reduced and the saccade, provided FEF and LIP still contain consistent plans, can be produced.

5. Discussion

This article describes how a rank-selective Item-and-Order spatial working memory (WM) can be used to represent arbitrary spatial sequences, and suggests that SEF is responsible for selecting spatial targets from WM and exciting corresponding representations in downstream oculomotor areas responsible for saccade production. Because it reproduces behavioral and electrophysiological data obtained through a variety of paradigms, including sequential and non-sequential oculomotor tasks, microstimulation studies, and electrophysiological mapping studies, the model makes testable predictions about the neural systems involved with storing spatial information and saccade generation. The following paragraphs review key model competencies, exploring ways in which they might suggest future directions of study.

5.1. Rank-selective working memory

One of the most important functionalities of the model is its ability to, for the first time within the Item-and-Order framework, simulate the storage and performance of sequences with repeated items at arbitrary list positions. By utilizing PPC representations of numerosity and rank (Nieder et al., 2006; Sawamura et al., 2002) to augment WM representations, as suggested by Grossberg and Pearson (2008), cues that appear at the same spatial position can be discriminated on the basis of their ordinal positions, and can therefore be stored in parallel in WM without interference. Our use of rank in both PFC and SEF is based on data showing that both of these heavily interconnected areas (Barbas & Pandya, 1987; Huerta & Kaas, 1990; Luppino, Rozzi, Calzavara, & Matelli, 2003) exhibit rank-selective activity (Averbeck et al., 2003; Berdyyeva & Olson, 2009; Isoda & Tanji, 2002, 2003). In our model, rank information in SEF is inherited from PFC activity, itself inherited from PPC. In fact, both regions receive projections from PPC (Petrides & Pandya, 1984; Rizzolatti et al., 1998), providing further support for the notion that rank-related activity originating in PPC might manipulate frontal populations.

Our model extends current observations about superior parietal lobule (SPL) counting cell activity, hypothesizing that it will track the rank of *cues* as they are presented, not just the rank of *actions* that occur sequentially, as was the case when the cells were first described (Sawamura et al., 2002). Though Nieder et al. (2006) did observe enumeration as cues were presented, further electrophysiological study is required to confirm the prediction that counting cells encode the rank of stimuli that appear in sequence. Should we observe this activity, a number of difficult questions must be asked: When does the counting cell population reset? Are all cues or only some (task-relevant) cues counted? Is a limited counting cell population bandwidth responsible for sequence length limitations observed in WM tasks? Moreover, results pertaining to rank-related activity often highlight cells with monotonically increasing or decreasing representations of rank (e.g. Averbeck et al., 2003), rather than broadly tuned activity centered about a specific preferred rank. Yet if rank-selective WM is, in fact, inherited from SPL counting cell activity, which shows broadly-tuned activity centered about a preferred rank, this type of activity should exist in PFC.

5.2. Working memory storage and item selection

The lisTELOS model clarifies how Item-Order-Rank spatial WM in PFC interacts with SEF to choose the next item for performance. The LIST PARSE model (Grossberg & Pearson, 2008) also distinguished WM storage from a subsequent stage of performance selection gated by the BG. Simulations were there given of WM storage of verbal lists by a cognitive WM in ventrolateral PFC, with item selection occurring in dorsolateral PFC. Simulations of arm movement sequences were also provided. Thus, verbal, spatial, and motor WMs may all use a similar neural circuit, as predicted by Grossberg (1978a). The lisTELOS model goes beyond LIST PARSE by simulating an Item-Order-Rank WM and frontal–parietal resonance in opening BG gates, among other advances. It remains to develop a unified theory for all of these WM and action systems.

5.3. Spatial working memory and coordinate systems

The model uses two different coordinate systems to represent spatial information: retinotopic, or eye-centered, and craniotopic, or head-centered, coordinate frames. Those areas responsible for processing inputs and shaping outputs use retinotopic coordinates because retinotopic coordinates facilitate the specification of oculomotor commands. WM and SEF selection use a craniotopic map of space to track progress throughout the entire sequence, without the need to remap with each saccade. By utilizing a representation which is stable throughout the entire motor sequence, these regions minimize processing related to the motor acts themselves. While there is evidence that cells in SEF use a craniotopic coordinate system (Bon & Lucchetti, 1990, Lee & Tehovnik, 1995, Schall, 1991, Sommer & Tehovnik, 1999 see also Olson & Gettner, 1995, 1999), current studies of PFC spatial WM only demonstrate that topography is present (Funahashi et al., 1989, 1990; Goldman-Rakic, 1996; Hagler & Sereno, 2006; Sawaguchi, 1996; Sawaguchi & Iba, 2001; Sawaguchi & Yamane, 1999), but not the coordinate frame being used (Rainer, Asaad, & Miller, 1998). Further study is required to determine if PFC spatial WM uses one or both of these topographies.

5.4. Basal ganglia gating of working memory

Our model uses the BG as a gating system (Alexander & Crutcher, 1990; Bullock & Grossberg, 1988, 1991; Gancarz & Grossberg, 1999; Grossberg et al., 1997; Hikosaka & Wurtz, 1983; Mink, 1996) that controls the flow of information between brain areas. Researchers have long hypothesized that the BG are responsible for controlling motor output from neurophysiological recordings (DeLong, 1971; Hikosaka et al., 1989; Hikosaka & Wurtz, 1983), by stimulation and inactivation of BG circuits (Denny-Brown & Yanagisawa, 1976; Hikosaka & Wurtz, 1983), and by the severe motor deficits incurred by Parkinson's and Huntington's diseases, which are associated with atypical BG structure and function (Albin, Young, & Penney, 1989; Wiecki & Frank, 2010). Although the various loops through the BG have been discussed and studied many times, with the exception of Grossberg (1978a, 1978b) wherein a rehearsal gate was posited, the notion that BG are important for moving information into and out of WM is relatively new (Cools, Sheridan, Jacobs, & D'Esposito, 2007; Frank et al., 2001; Grossberg & Pearson, 2008; O'Reilly & Frank, 2006).

The model uses the BG to control the flow of spatial information from WM circuits to SEF, and indeed the rest of the oculomotor system. Gating of WM output provides a simple mechanism for withholding motor output by only allowing information to flow between cortical areas when task conditions permit sequence reproduction. Stocco, Lebiere, and Anderson (2010) have described how the BG can perform this process, called *conditional routing*. Our inclusion of a gate controlling WM output supports the growing body of evidence suggesting that BG play an important role in the control of this process.

5.5. Supplementary eye field as a selection system

The model SEF is the most expanded model area, with more cell populations than any other region (Figs. 1 and 18), and with a focus on manipulation of the area's activity following microstimulation. Since SEF selects items from an Item-Order-Rank WM, it must be able to handle rank-sensitive representations. SEF is known to contain cells with rank-dependent activity (Berdyyeva & Olson, 2009; Isoda & Tanji, 2002, 2003), and has been thought to play a critical role in the production of memory-guided saccade sequences (Gaymard et al., 1990, 1993; Schiller & Chou, 1998; Sommer & Tehovnik, 1999). SEF experiments describe phasic bursts of activity prior to the initiation of saccades (Isoda & Tanji, 2002, 2003; Lu et al., 2002), providing further evidence that SEF helps to extract rank-sensitive saccade plans from sequential WM and initiate saccade production. Our use of SEF also clarifies recent suggestions that SEF is involved with conflict resolution or action selection (Nachev et al., 2005; Parton et al., 2007; So & Stuphorn, 2010; Taylor et al., 2007). Our proposal that SEF selects saccade plans is, furthermore, supported by model simulation of SEF microstimulation data. In summary, the model unifies the explanation of a variety of data that have for years hinted at the region's function, but have never been clear or consistent enough to provide definitive answers. The debates surrounding the coordinate frame of the region's topographical organization serve as an excellent example of the confusion that accompanies most SEF investigations: Although evidence for a craniotopic organization seems strongest, there is no shortage of results suggesting retinotopic, or even object-centered representations.

SEF cells also undergo learning-related changes in their response properties (Chen & Wise, 1995a, 1995b, 1996; Mann et al., 1988). If SEF is simply choosing the strongest WM representation, what is it learning? If the job of SEF truly is to select plans from WM, could such changes in organization follow similar changes in PFC representations, notably the learning of sequential plans (Grossberg & Pearson, 2008)? Future investigations of SEF should examine how the representational scheme encountered in SEF changes as a function of the environment, of task demands, and of changes in other cortical areas with which SEF is interconnected. Though there seems to be more to SEF than a competitive network, our simulations suggest such an explanation may provide a solid foundation upon which to explain the area's more nuanced properties.

Acknowledgments

Supported in part by CELEST, an NSF Science of Learning Center (SBE-0354378) and by the DARPA SyNAPSE program (HR0011-09-C-0001).

References

Albin, R. L., Young, A. B., & Penney, J. B. (1989). The functional anatomy of basal ganglia disorders. *Trends in Neurosciences*, *12*, 366–375.

Alexander, G. E., & Crutcher, M. D. (1990). Functional architecture of basal ganglia circuits: neural substrates of parallel processing. *Trends in Neurosciences*, *1*(3), 266–271.

Andersen, R., Essick, G., & Siegel, R. (1987). Neurons of area 7 activated by both visual stimuli and oculomotor behavior. *Experimental Brain Research*, *67*(2), 316–322.

Averbeck, B., Chafee, M., Crowe, D., & Georgopoulos, A. (2002). Parallel processing of serial movements in prefrontal cortex. *Proceedings of the National Academy of Sciences of the United States of America*, *99*(20), 13172–13177.

Averbeck, B., Chafee, M., Crowe, D., & Georgopoulos, A. (2003). Neural activity in prefrontal cortex during copying geometrical shapes. I. Single cells encode shape, sequence, and metric parameters. *Experimental Brain Research*, *150*(2), 127–141.

Awh, E., & Vogel, E. K. (2008). The bouncer in the brain. *Nature Neuroscience*, *11*(1), 5–6.

Barbas, H., & Pandya, D. (1987). Architecture and frontal cortical connections of the premotor cortex(area 6) in the rhesus monkey. *The Journal of Comparative Neurology*, *256*(2), 211–228.

Barone, P., & Joseph, J. (1989). Prefrontal cortex and spatial sequencing in macaque monkey. *Experimental Brain Research*, *78*(3), 447–464.

Berdyyeva, T., & Olson, C. (2009). Monkey supplementary eye field neurons signal the ordinal position of both actions and objects. *Journal of Neuroscience*, *29*(3), 591.

Bisley, J., Krishna, B., & Goldberg, M. (2004). A rapid and precise on-response in posterior parietal cortex. *Journal of Neuroscience*, *24*(8), 1833–1838.

Bizzi, E. (1968). Discharge of frontal eye field neurons during saccadic and following eye movements in unanesthetized monkeys. *Experimental Brain Research*, *6*(1), 69–80.

Boardman, I., & Bullock, D. (1991). A neural network model of serial order recall from short-term memory. Paper presented at *The international joint conference on neural networks. Seattle. Vol. 2* (pp. 879–884).

Bohland, J., Bullock, D., & Guenther, F. (2010). Neural representations and mechanisms for the performance of simple speech sequences. *Journal of Cognitive Neuroscience*, *22*(7), 1504–1529.

Bon, L., & Lucchetti, C. (1990). Does attention affect the motor programs of pharmacologically induced eye movements? *International Journal of Neuroscience*, *53*(2–4), 103–109.

Bowman, H., & Wyble, B. (2007). The simultaneous type, serial token model of temporal attention and working memory. *Psychological Review*, *114*(1), 38–70.

Bradski, G., Carpenter, G., & Grossberg, S. (1994). STORE working memory networks for storage and recall of arbitrary temporal sequences. *Biological Cybernetics*, *71*(6), 469–480.

Brannon, E., & Terrace, H. (1998). Ordering of the numerosities 1 to 9 by monkeys. *Science*, *282*(5389), 746–749.

Brannon, E., & Terrace, H. (2000). Representation of the numerosities 1–9 by rhesus macaques (macaca mulatta). *Journal of Experimental Psychology: Animal Behavior Processes*, *26*(1), 31–49.

Brown, J., Bullock, D., & Grossberg, S. (2004). How laminar frontal cortex and basal ganglia circuits interact to control planned and reactive saccades. *Neural Networks*, *17*, 471–510.

Brown, G., Preece, T., & Hulme, C. (2000). Oscillator-based memory for serial order. *Psychological Review*, *107*(1), 127–181.

Bruce, C., & Goldberg, M. (1985). Primate frontal eye fields. I. Single neurons discharging before saccades. *Journal of Neurophysiology*, *53*(3), 603–635.

Bruce, C., Goldberg, M., Bushnell, M., & Stanton, G. (1985). Primate frontal eye fields. II. Physiological and anatomical correlates of electrically evoked eye movements. *Journal of Neurophysiology*, *54*(3), 714–735.

Bullock, D., & Grossberg, S. (1988). Neural dynamics of planned arm movements: emergent invariants and speed-accuracy properties during trajectory formation. *Psychological Review*, *95*, 49–90.

Bullock, D., & Grossberg, S. (1991). Adaptive neural networks for control of movement trajectories invariant under speed and force rescaling. *Human Movement Science*, *10*(1), 3–53.

Bullock, D., & Rhodes, B. (2003). Competitive queuing for planning and serial performance. In M. Arbib (Ed.), *Handbook of brain theory and neural networks* (2nd ed.) (pp. 241–244). Cambridge, MA: MIT Press.

Burgess, N., & Hitch, G. (1999). Memory for serial order: a network model of the phonological loop and its timing. *Psychological Review*, *106*, 551–581.

Buschman, T. J., & Miller, E. K. (2007). Top–down versus bottom-up control of attention in the prefrontal and posterior parietal cortices. *Science*, *315*, 1860–1862.

Chen, L., & Wise, S. (1995a). Neuronal activity in the supplementary eye field during acquisition of conditional oculomotor associations. *Journal of Neurophysiology*, *73*(3), 1101–1121.

Chen, L., & Wise, S. (1995b). Supplementary eye field contrasted with the frontal eye field during acquisition of conditional oculomotor associations. *Journal of Neurophysiology*, *73*(3), 1122–1134.

Chen, L., & Wise, S. (1996). Evolution of directional preferences in the supplementary eye field during acquisition of conditional oculomotor associations. *Journal of Neuroscience*, *16*(9), 3067–3081.

Colby, C., Duhamel, J., & Goldberg, M. (1996). Visual, presaccadic, and cognitive activation of single neurons in monkey lateral intraparietal area. *Journal of Neurophysiology*, *76*(5), 2841–2852.

Conrad, R. (1960). Serial order intrusions in immediate memory. *British Journal of Psychology*, *51*(1), 45.

Cools, R., Sheridan, M., Jacobs, E., & D'Esposito, M. (2007). Impulsive personality predicts dopamine-dependent changes in frontostriatal activity during component processes of working memory. *Journal of Neuroscience*, *27*(20), 5506–5514.

Dehaene, S. (1997). *The number sense: how the mind creates mathematics*. New York, NY: Oxford University Press.

Dehaene, S., Spelke, E., Pinel, P., Stenescu, R., & Tsivkin, S. (1999). Sources of mathematical thinking: behavioral and brain-imaging evidence. *Science*, *284*, 970–974.

DeLong, M. R. (1971). Activity of pallidal neurons during movement. *Journal of Neurophysiology*, *34*, 414–427.

Denny-Brown, D., & Yanagisawa, N. (1976). The role of the basal ganglia in the initiation of movement. In M. D. Yahr (Ed.), *The basal ganglia* (pp. 115–149). New York, NY: Raven Press.

Droulez, J., & Berthoz, A. (1991). A neural network model of sensoritopic maps with predictive short-term memory properties. *Proceedings of the National Academy of Sciences of the United States of America*, *88*(21), 9653.

Farrell, S., & Lewandowsky, S. (2004). Modelling transposition latencies: constraints for theories of serial order memory. *Journal of Memory and Language*, *51*(1), 115–135.

Fazl, A., Grossberg, S., & Mingolla, E. (2009). View-invariant object category learning, recognition, and search: how spatial and object attention are coordinated using surfacebased attentional shrouds. *Cognitive Psychology*, *58*(1), 1–48.

Frank, M. J. (2005). Dynamic dopamine modulation in the basal ganglia: a neurocomputational account of cognitive deficits in medicated and non-medicated parkinsonism. *Journal of Cognitive Neuroscience*, *17*, 51–72.

Frank, M. J., Loughry, B., & O'Reilly, R. C. (2001). Interactions between the frontal cortex and basal ganglia in working memory: a computational model. *Cognitive, Active & Behavioral Neuroscience*, *1*, 137–160.

Funahashi, S., Bruce, C., & Goldman-Rakic, P. (1989). Mnemonic coding of visual space in the monkey's dorsolateral prefrontal cortex. *Journal of Neurophysiology*, *61*(2), 331–349.

Funahashi, S., Bruce, C., & Goldman-Rakic, P. (1990). Visuospatial coding in primate prefrontal neurons revealed by oculomotor paradigms. *Journal of Neurophysiology*, *63*(4), 814–831.

Fuster, J. M. (1973). Unit activity in prefrontal cortex during delayed-response performance: neuronal correlates of transient memory. *Journal of Neurophysiology*, *36*(1), 61–78.

Gancarz, G., & Grossberg, S. (1999). A neural model of the saccadic eye movement control explains task-specific adaptation. *Vision Research*, *39*, 3123–3143.

Gaudiano, P., & Grossberg, S. (1991). Vector associative maps: unsupervised real-time error-based learning and control of movement trajectories. *Neural Networks*, *4*, 147–183.

Gaymard, B., Pierrot-Deseilligny, C., & Rivaud, S. (1990). Impairment of sequences of memory-guided saccades after supplementary motor area lesions. *Annals of Neurology*, *28*(5), 622–626.

Gaymard, B., Ploner, C., Rivaud-Pechoux, S., & Pierrot-Deseilligny, C. (1999). The frontal eye field is involved in spatial short-term memory but not in reflexive saccade inhibition. *Experimental Brain Research*, *129*(2), 288–301.

Gaymard, B., Rivaud, S., & Pierrot-Deseilligny, C. (1993). Role of the left and right supplementary motor areas in memory-guided saccade sequences. *Annals of Neurology*, *34*(3), 404–406.

Gerfen, C. R., Engber, T. M., Mahan, L. C., Susel, Z., Chase, T. N., Monsama, F. J., et al. (1990). D1 and D2 dopamine receptor-regulated gene expression of striatonigral and striatopallidal neurons. *Science*, *250*(4986), 1429–1432.

Goldberg, M., & Bushnell, M. (1981). Behavioral enhancement of visual responses in monkey cerebral cortex. II. Modulation in frontal eye fields specifically related to saccades. *Journal of Neurophysiology*, *46*(4), 773–787.

Goldman-Rakic, P. (1996). Regional and cellular fractionation of working memory. *Proceedings of the National Academy of Sciences of the United States of America*, *93*(24), 13473–13480.

Grossberg, S. (1968). Some physiological and biochemical consequences of psychological postulates. *Proceedings of the National Academy of Sciences of the United States of America*, *60*(3), 758–765.

Grossberg, S. (1970). Neural pattern discrimination. *Journal of Theoretical Biology*, *27*, 291–337.

Grossberg, S. (1972). A neural theory of punishment and avoidance, II: quantitative theory. *Mathematical Biosciences*, *15*, 253–285.

Grossberg, S. (1973). Contour enhancement, short term memory, and constancies in reverberating neural networks. *Studies in Applied Mathematics*, *52*(3), 213–257.

Grossberg, S. (1978a). A theory of human memory: self-organization and performance of sensory-motor codes, maps, and plans. In R. Rosen, & F. Snell (Eds.), *On progress in theoretical biology*: *Vol. 5* (pp. 233–374). New York: Academic Press.

Grossberg, S. (1978b). Behavioral contrast in short term memory: serial binary memory models or parallel continuous memory models. *Journal of Mathematical Psychology*, *17*(3), 199–219.

Grossberg, S., & Kuperstein, M. (1989). *Neural dynamics of adaptive sensory-motor control* (expanded ed.) Elmsford, NY: Pergamon Press (Chapter 10).

Grossberg, S., & Pearson, L. (2008). Laminar cortical dynamics of cognitive and motor working memory, sequence learning and performance: toward a unified theory of how the cerebral cortex works. *Psychological Review*, *115*(3), 677–732.

Grossberg, S., & Repin, D. V. (2003). A neural model of how the brain represents and compares multi-digit numbers: spatial and categorical processes. *Neural Networks*, *16*, 1107–1140.

Grossberg, S., Roberts, K., Aguilar, M., & Bullock, D. (1997). A neural model of multimodal adaptive saccadic eye movement control by superior colliculus. *Journal of Neuroscience*, *17*, 9706–9725.

Hagler, D., & Sereno, M. (2006). Spatial maps in frontal and prefrontal cortex. *NeuroImage*, *29*(2), 567–577.

Hanes, D., Thompson, K., & Schall, J. (1995). Relationship of presaccadic activity in frontal eye field and supplementary eye field to saccade initiation in macaque: Poisson spike train analysis. *Experimental Brain Research*, *103*(1), 85–96.

Heide, W., Binkofski, F., Seitz, R., Posse, S., Nitschke, M., Freund, H., et al. (2001). Activation of frontoparietal cortices during memorized triple-step sequences of saccadic eye movements: an fMRI study. *European Journal of Neuroscience*, *13*(6), 1177–1189.

Henson, R. N. A. (1998). Short-term memory for serial order: the start-end model. *Cognitive Psychology*, *36*, 73–137.

Henson, R. N. A. (2001). Serial order in short-term memory. *The Psychologist*, *14*(2), 70–73.

Hikosaka, O., Sakamoto, M., & Usui, S. (1989). Functional properties of monkey caudate neurons. I. Activities related to saccadic eye movements. *Journal of Neurophysiology*, *61*(4), 780–798.
Hikosaka, O., & Wurtz, R. H. (1983). Visual and oculomotor functions of monkey substantia nigra pars reticulata. IV. Relation of substantia nigra to superior colliculus. *Journal of Neurophysiology*, *49*, 1285–1301.
Hikosaka, O., & Wurtz, R. H. (1989). The basal ganglia. In R. Wurtz, & M. Goldberg (Eds.), *The neurobiology of saccadic eye movements* (pp. 257–281). Amsterdam: Elsevier.
Histed, M. H., Bonin, V., & Reid, R. C. (2009). Direct activation of sparse, distributed populations of cortical neurons by electrical microstimulation. *Neuron*, *63*(4), 508–522.
Histed, M. H., & Miller, E. K. (2006). Microstimulation of frontal cortex can reorder a remembered spatial sequence. *Public Library of Science: Biology*, *4*(5), e134.
Hodgkin, A. L. (1964). *The conduction of the nerve impulse*. Springfield, Illinois: Thomas.
Horak, F. B., & Anderson, M. E. (1984). Influence of globus pallidus on arm movements in monkeys, II. Effects of stimulation. *Journal of Neurophysiology*, *52*, 305–322.
Houghton, G. (1990). The problem of serial order: a neural network model of sequence learning and recall. In *Cognitive science series* (pp. 287–319). Academic Press.
Huerta, M., & Kaas, J. (1990). Supplementary eye field as defined by intracortical microstimulation: connections in macaques. *The Journal of Comparative Neurology*, *293*, 299–330.
Isoda, M., & Tanji, J. (2002). Cellular activity in the supplementary eye field during sequential performance of multiple saccades. *Journal of Neurophysiology*, *88*, 3541–3545.
Isoda, M., & Tanji, J. (2003). Contrasting neuronal activity in the supplementary and frontal eye fields during temporal organization of multiple saccades. *Journal of Neurophysiology*, *90*(5), 3054–3065.
Jin, Z., & Reeves, A. (2009). Attentional release in the saccadic gap effect. *Vision Research*, *49*(16), 2045–2055.
Kojima, S., & Goldman-Rakic, P. S. (1984). Functional analysis of spatially discriminative neurons in prefrontal cortex of rhesus monkey. *Brain Research*, *291*(2), 229–240.
Lashley, K. (1951). The problem of serial order in behavior. In L. A. Jeffress (Ed.), *Cerebral mechanisms in behavior* (pp. 112–131). New York: Wiley.
Lee, C., Rohrer, W., & Sparks, D. (1988). Population coding of saccadic eye movements by neurons in the superior colliculus. *Nature*, *332*(6162), 357–360.
Lee, K., & Tehovnik, E. J. (1995). Topographic distribution of fixation-related units in the dorsomedial frontal cortex of the rhesus monkey. *European Journal of Neuroscience*, *7*, 1005–1011.
Lu, X., Matsuzawa, M., & Hikosaka, O. (2002). A neural correlate of oculomotor sequences in supplementary eye field. *Neuron*, *34*(2), 317–325.
Luppino, G., Rozzi, S., Calzavara, R., & Matelli, M. (2003). Prefrontal and agranular cingulate projections to the dorsal premotor areas f2 and f7 in the macaque monkey. *European Journal of Neuroscience*, *17*(3), 559–578.
Mann, S., Thau, R., & Schiller, P. (1988). Conditional task-related responses in monkey dorsomedial frontal cortex. *Experimental Brain Research*, *69*(3), 460–468.
McNab, F., & Klingberg, T. (2008). Prefrontal cortex and basal ganglia control access to working memory. *Nature Neuroscience*, *11*, 103–107.
Middleton, F., & Strick, P. (2000). Basal ganglia and cerebellar loops: motor and cognitive circuits. *Brain Research Reviews*, *31*, 236–250.
Mink, J. (1996). The basal ganglia: focused selection and inhibition of competing motor programs. *Progress in Neurobiology*, *50*(4), 381–425.
Mitchell, J., & Zipser, D. (2003). Sequential memory-guided saccades and target selection: a neural model of the frontal eye fields. *Vision Research*, *43*(25), 2669–2695.
Munoz, D., & Wurtz, R. (1993). Fixation cells in monkey superior colliculus. I. Characteristics of cell discharge. *Journal of Neurophysiology*, *70*(2), 559–575.
Munoz, D., & Wurtz, R. (1995). Saccade-related activity in monkey superior colliculus. I. Characteristics of burst and buildup cells. *Journal of Neurophysiology*, *73*(6), 2313–2333.
Mushiake, H., Saito, N., Sakamoto, K., Itoyama, Y., & Tanji, J. (2006). Activity in the lateral prefrontal cortex reflects multiple steps of future events in action plans. *Neuron*, *50*(4), 631–641.
Nachev, P., Rees, G., Parton, A., Kennard, C., & Husain, M. (2005). Volition and conflict in human medial frontal cortex. *Current Biology*, *15*(2), 122–128.
Nieder, A., Diester, I., & Tudusciuc, O. (2006). Temporal and spatial enumeration processes in the primate parietal cortex. *Science*, *313*, 1431–1435.
Nieder, A., & Miller, E. (2004a). Analog numerical representations in rhesus monkeys: evidence for parallel processing. *Journal of Cognitive Neuroscience*, *16*(5), 889–901.
Nieder, A., & Miller, E. (2004b). A parieto-frontal network for visual numerical information in the monkey. *Proceedings of the National Academy of Sciences of the United States of America*, *101*(19), 7457–7462.
Olson, C., & Gettner, S. (1995). Object-centered direction selectivity in the macaque supplementary eye field. *Science*, *269*(5226), 985–988.
Olson, C., & Gettner, S. (1999). Macaque SEF neurons encode object-centered directions of eye movements regardless of the visual attributes of instructional cues. *Journal of Neurophysiology*, *81*(5), 2340–2346.
Olson, C., & Tremblay, L. (2000). Macaque supplementary eye field neurons encode object-centered locations relative to both continuous and discontinuous objects. *Journal of Neurophysiology*, *83*(4), 2392–2411.
O'Reilly, R. C., & Frank, M. J. (2006). Making working memory work: a computational model of learning in the prefrontal cortex and basal ganglia. *Neural Computation*, *18*, 283–328.
Ottes, F., Van Gisbergen, J., & Eggermont, J. (1984). Metrics of saccade responses to visual double stimuli: two different modes. *Vision Research*, *24*(10), 1169–1179.
Ozyurt, J., Rutschmann, R., & Greenlee, M. (2006). Cortical activation during memory-guided saccades. *NeuroReport*, *17*(10), 1005–1009.
Page, M., & Norris, D. (1998). The primacy model: a new model of immediate serial recall. *Psychological Review*, *105*(4), 761–781.
Park, J., Schlag-Rey, M., & Schlag, J. (2006). Frames of reference for saccadic command tested by saccade collision in the supplementary eye field. *Journal of Neurophysiology*, *95*(1), 159–170.
Parton, A., Nachev, P., Hodgson, T., Mort, D., Thomas, D., Ordrige, R., et al. (2007). Role of the human supplementary eye field in the control of saccadic eye movements. *Neuropsychologia*, *45*(5), 997–1008.
Petit, L., Orssaud, C., Tzourio, N., Crivello, F., Berthoz, A., & Mazoyer, B. (1996). Functional anatomy of a prelearned sequence of horizontal saccades in humans. *Journal of Neuroscience*, *16*(11), 3714–3726.
Petrides, M., & Pandya, D. (1984). Projections to the frontal cortex from the posterior parietal region in the rhesus monkey. *The Journal of Comparative Neurology*, *228*(1), 105–116.
Pratt, J., Bekkering, H., Abrams, R., & Adam, J. (1999). The gap effect for spatially oriented responses. *Acta Psychologica*, *102*(1), 1–12.
Rainer, G., Asaad, W. F., & Miller, E. K. (1998). Selective representation of relevant information by neurons in the primate prefrontal cortex. *Nature*, *393*(6685), 577–578.
Rizzolatti, G., Luppino, G., & Matelli, M. (1998). The organization of the cortical motor system: new concepts. *Electroencephalography and Clinical Neurophysiology*, *106*(4), 283–296.
Robinson, D., & Fuchs, A. (1969). Eye movements evoked by stimulation of frontal eye fields. *Journal of Neurophysiology*, *32*(5), 637–648.
Roitman, J., Brannon, E., & Platt, M. (2007). Monotonic coding of numerosity in macaque lateral intraparietal area. *Public Library of Science: Biology*, *5*(8), e208.
Saslow, M. (1967). Effects of components of displacement-step stimuli upon latency for saccadic eye movement. *Journal of the Optical Society of America*, *57*(8), 1024–1029.
Sawaguchi, T. (1996). Functional modular organization of the primate prefrontal cortex for representing working memory process. *Cognitive Brain Research*, *5*(1–2), 157–163.
Sawaguchi, T., & Iba, M. (2001). Prefrontal cortical representation of visuospatial working memory in monkeys examined by local inactivation with muscimol. *Journal of Neurophysiology*, *86*(4), 2041–2053.
Sawaguchi, T., & Yamane, I. (1999). Properties of delay-period neuronal activity in the monkey dorsolateral prefrontal cortex during a spatial delayed matching-to-sample task. *Journal of Neurophysiology*, *82*(5), 2070–2080.
Sawamura, H., Shima, K., & Tanji, J. (2002). Numerical representation for action in the parietal cortex of the monkey. *Nature*, *415*(6874), 918–922.
Saygin, A., & Sereno, M. (2008). Retinotopy and attention in human occipital, temporal, parietal, and frontal cortex. *Cerebral Cortex*, *18*, 2158–2168.
Schall, J. D. (1991). Neuronal activity related to visually guided saccades in the frontal eye fields of rhesus monkeys: comparison with supplementary eye fields. *Journal of Neurophysiology*, *66*(2), 559–579.
Schiller, P., & Chou, I. (1998). The effects of frontal eye field and dorsomedial frontal cortex lesions on visually guided eye movements. *Nature Neuroscience*, *1*, 248–253.
Schlag, J., & Schlag-Rey, M. (1987). Evidence for a supplementary eye field. *Journal of Neurophysiology*, *57*(1), 179–200.
Shook, B., Schlag-Rey, M., & Schlag, J. (1991). Primate supplementary eye field. II. Comparative aspects of connections with the thalamus, corpus striatum, and related forebrain nuclei. *The Journal of Comparative Neurology*, *307*, 562–583.
So, N., & Stuphorn, V. (2010). Supplementary eye field encodes option and action value for saccades with variable reward. *Journal of Neurophysiology*, *104*, 2634–2653.
Sommer, M., & Tehovnik, E. (1999). Reversible inactivation of macaque dorsomedial frontal cortex: effects on saccades and fixations. *Experimental Brain Research*, *124*(4), 429–446.
Sparks, D., Holland, R., & Guthrie, B. (1976). Size and distribution of movement fields in the monkey superior colliculus. *Brain Research*, *113*(1), 21–34.
Stocco, A., Lebiere, C., & Anderson, J. R. (2010). Conditional routing of information to the cortex: a model of the basal ganglia's role in cognitive coordination. *Psychological Review*, *117*(2), 540–574.
Surmeier, D. J., Ding, J., Day, M., Wang, Z., & Shen, W. (2007). D1 and D2 dopamine-receptor modulation of striatal glutamatergic signaling in striatal medium spiny neurons. *Trends in Neurosciences*, *30*(5), 228–235.
Taylor, P., Nobre, A., & Rushworth, M. (2007). Subsecond changes in top down control exerted by human medial frontal cortex during conflict and action selection: a combined transcranial magnetic stimulation electroencephalography study. *Journal of Neuroscience*, *27*(42), 11343–11353.
Tremblay, L., Gettner, S., & Olson, C. (2002). Neurons with object-centered spatial selectivity in macaque SEF: do they represent locations or rules? *Journal of Neurophysiology*, *87*(1), 333–350.
Tsushima, Y., Seitz, A. R., & Watanabe, T. (2008). Task-irrelevant learning occurs only when the irrelevant feature is weak. *Current Biology*, *18*(12), R516–R517.
Warden, M. R., & Miller, E. K. (2010). Task-dependent changes in short-term memory in the prefrontal cortex. *The Journal of Neuroscience*, *30*(47), 15801–15810.

Wiecki, T. V., & Frank, M. J. (2010). Neurocomputational models of motor and cognitive deficits in Parkinson's disease. *Progress in Brain Research*, *183*, 275–297.

Wurtz, R., & Goldberg, M. (1972). Activity of superior colliculus in behaving monkey. 3. Cells discharging before eye movements. *Journal of Neurophysiology*, *35*(4), 575–586.

Yang, S., Heinen, S., & Missal, M. (2008). The effects of microstimulation of the dorsomedial frontal cortex on saccade latency. *Journal of Neurophysiology*, *99*(4), 1857–1870.

Zipser, D., & Andersen, R. (1988). A back-propagation programmed network that simulates response properties of a subset of posterior parietal neurons. *Nature*, *331*(6158), 679–684.